



## What else should hemostatic materials do beyond hemostasis: A review

Xinran Yang<sup>a,b,c,1</sup>, Xiudan Wang<sup>a,b,c,1</sup>, Xing Gao<sup>a,d</sup>, Xiaoqin Guo<sup>a,b,c</sup>, Shike Hou<sup>a,b,c,\*\*</sup>,  
Jie Shi<sup>a,b,c,\*\*\*</sup>, Qi Lv<sup>a,b,c,\*</sup>

<sup>a</sup> Institution of Disaster and Emergency Medicine, Tianjin University, Tianjin 300072, China

<sup>b</sup> Key Laboratory for Disaster Medicine Technology, Tianjin 300072, China

<sup>c</sup> Wenzhou Safety (Emergency) Institute of Tianjin University, Wenzhou 325026, China

<sup>d</sup> Tianjin Hospital, Tianjin 300072, China

### ARTICLE INFO

#### Keywords:

Massive blood loss  
Hemostatic material  
Rapid hemostasis  
Noncompressible bleeding  
Wound healing

### ABSTRACT

Massive blood loss due to injury is the leading cause of prehospital deaths in disasters and emergencies. Hemostatic materials are used to realize rapid hemostasis and protect patients from death. Researchers have designed and developed a variety of hemostatic materials. However, in addition to their hemostatic effect, hemostatic materials must be endowed with additional functions to meet the practical application requirements in different scenarios. Here, strategies for modifications of hemostatic materials for use in different application scenarios are listed: effective positioning at the site of deep and narrow wounds to stop bleeding, resistance to high blood pressure and wound movement to maintain wound formation, rapid and easy removal from the wound without affecting further treatment after hemostasis is completed, and continued function when retained in the wound as a dressing (such as antibacterial, antiadhesion, tissue repair, etc.). The problems encountered in the practical use of hemostatic materials and the strategies and progress of researchers will be further discussed in this review. We hope to provide valuable references for the design of more comprehensive and practical hemostatic materials.

### 1. Introduction

Disaster events and emergencies are prone to cause external trauma to the human body, which is associated with a high risk of death. Massive blood loss is the most important factor in prehospital deaths [1]. Loss of more than one third of the blood in the body induces a series of systemic reactions, such as deep coma and shock. Studies have shown that if bleeding can be controlled within 60 min, the survival rate of the injured individual increases by 20–30% [2]. For important viscera, artery rupture hemorrhage or bleeding can occur in the limbs and trunk of the phase boundary between parts of an oppressive bleeding event, simply using a tourniquet or gauze cannot work [3]. Rapid surgery is needed, but the absence of on-site medical conditions may mean there is no effective treatment for the wounded. Therefore, to minimize the likelihood of early death, it is necessary to intervene quickly after the injury and stop bleeding caused by trauma.

A variety of hemostatic materials have been certified and widely used in various scenarios. QuikClot® combat gauze [76], CELOX® hemostatic powder [77], XSTAT® compression sponge [78] and other products have been deployed by the U.S. Army. These products act directly on the wound site and quickly stop bleeding. Early inhibition of internal bleeding, early inhibition can be achieved by oral or intravenous administration of tranexamic acid (TXA) [79]. However, more urgent problems arise during the use of these materials: dressings or powder-based materials cannot be easily removed from the wound after hemostasis; adhesion to wounds or moist environments *in vivo* is poor; and it is difficult to deal with large artery bleeding without external force.

In addition to the hemostatic effect, hemostatic materials must also have new functions to meet the needs of rapid hemostasis. Moreover, the functions of hemostatic materials for different wounds on the body surface or internal organs also differ. For diffuse bleeding and tissue/

\* Corresponding author. Institution of Disaster and Emergency Medicine, Tianjin University, Tianjin 300072, China.

\*\* Corresponding author. Institution of Disaster and Emergency Medicine, Tianjin University, Tianjin 300072, China.

\*\*\* Corresponding author. Institution of Disaster and Emergency Medicine, Tianjin University, Tianjin 300072, China.

E-mail addresses: [housk86@163.com](mailto:housk86@163.com) (S. Hou), [shijieland@126.com](mailto:shijieland@126.com) (J. Shi), [lvqi@tju.edu.cn](mailto:lvqi@tju.edu.cn) (Q. Lv).

<sup>1</sup> Xinran Yang and Xiudan Wang contributed equally to the article.

organ injury in the body, for hemostatic materials must quickly reach the bleeding site, protect the wound morphology, promote wound healing and harmlessly degrade. For external surface wounds or open wounds, the focus is on rapid removal of hemostatic materials for further care after hemostasis, or the hemostatic materials are expected to remain around the wound in the form of dressings to provide long-term support. Thus, we summarize these improvement strategies into the following four categories (Fig. 1): 1. Positioning on the bleeding site; 2. Mechanical strength sufficient to resist internal and external pressure; 3. Easy removal or rapid degradation in the short term after hemostasis is completed; 4. Anti-adhesion, antibacteria, tissue repair and other effects if the material is retained in the wound for a long time after hemostasis. Traditional hemostatic materials are often unable to provide all of these effects. Some materials with excellent hemostatic effects, such as fibrin glue, are considered to be too expensive and do not have the tensile strength required to maintain the wound site [80,81]; materials with good mechanical strength such as cyanoacrylate may lack biological safety [82].

There have been many reviews on the explorations of these materials and hemostatic mechanisms. Therefore, in this review, we paid more attention to the other functions that should be considered in addition to the hemostatic effect of the material itself in order to better achieve the basic goals of rapid hemostasis and treatment effectively. We comprehensively reviewed the existing hemostatic materials while focusing on the improvement strategies and progress in the latest research on existing hemostatic materials in terms of positioning, maintenance, rapid removal and sustained action. Finally, we propose further development directions for hemostatic materials, hoping to improve the existing hemostatic materials through high-throughput sequencing screening and modular design, so that they can be more suitable for the actual rescue situations and promote the transformation of laboratory research into actual products.

## 2. Positioning the material on the bleeding site

Positioning of the material at the bleeding site is an inevitable problem in the research of hemostatic materials. Normally hemostatic materials are maintained around the wounds by adhesion or pressure, where they form an initial physical hemostatic barrier and trigger the coagulation cascade [83]. If the adhesion is strong enough, hemostatic

material can first block the vessel and stop blood flow to achieve preliminary hemostasis. For complex bleeding wounds, especially noncompressible bleeding wounds *in vivo*, it is difficult to apply traditional hemostatic materials at the bleeding site. The humid and dynamic environment formed by blood and tissue fluid covering the bleeding site also poses challenges for material's adhesion. Several studies have improved the bonding methods of materials, such as rapid underwater/wet adhesion, mechanical interlocking, *in vivo* targeted guidance, and self-propulsion/magnetic field guidance, to facilitate the combination of materials and wounds (Fig. 2 and Table 1).

### 2.1. Wet adhesion

Materials such as hydrogels contact with adhesive interfaces through various molecular interactions to form tight adhesion, including metal coordination bonds [84], covalent bonds [85], van der Waals forces [86], and hydrogen bonds [87]. However, the presence of interfacial water in the wet state environment weakens the interactions between the material functional groups and the tissue interface. Robust wet-tissue adhesion capability is the primary task.

Inspired by the structures of mussel foot proteins (mfps), researchers have introduced catechol which contains polydopamine (PDA), into hydrogels to significantly improve the adhesion of the hydrogel material in the wet environments [88]. Li et al. [4] designed a series of cryogels for rapid noncompressible hemostasis based on quaternary ammonium chitosan and polydopamine. With the help of a large number of positively charged amino groups, quaternary ammonium groups and catechol groups, the adhesion strength of the material reached up to 24.0 kPa, and increased to more than 50.9 kPa after 30 min. The macroporous structure of the cryogel also provided a larger contact area between the tissue and the cryogel to further strengthen adhesion. Wu et al. [5] grafted dopamine to aldehyde-based chondroitin sulfate (OHC-CSA) and chemically polymerized it with carboxymethyl chitosan to form a hydrogel. The highest adhesion strength of the hydrogel in the porcine skin inner layer-inner layer adhesion model was 0.72 MPa.

Another challenge for adhesion in the wet state is the need to quickly exclude the interfacial water between the material and the tissue, which allows the material to adhere effectively to the tissue interface. Pan et al. [6] reported the introduction of Ag nanoparticles and decellularized extracellular matrix (dECM) into a bionic catechol-conjugated chitosan

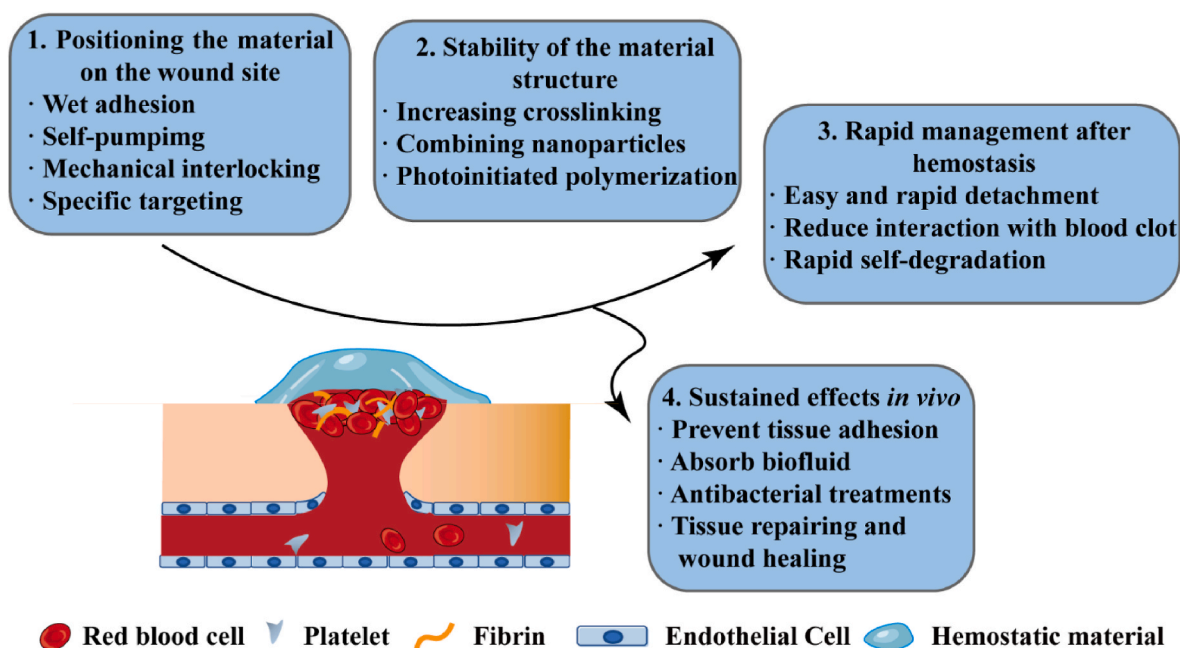


Fig. 1. Four additional functions in the application of hemostatic materials.

**Table 1**  
Summary of measures to improve the positioning of hemostatic materials to the bleeding site.

Name	Material Components	Improved properties	Main models and hemostasis time	Reference
QCS/PDA cryogels	Quaternized chitosan and polydopamine	Adhesion strength: 24.0 kPa and over 50.9 kPa after 30 min.	Rat liver injury: about 60 s; Rabbit Liver Volume Defect: 188 s.	[4]
SA-DA-CS hydrogel	Dopamine-grafted oxidized chondroitin sulfate and carboxymethyl chitosan	Adhesion strength: up to 0.72 MPa.	Rat liver injury: 1.5 min.	[5]
C-CTS/SA-Ag/dECM composite hydrogel	Catechol-conjugated chitosan, tannic acid, silk fibroin, Ag NPs and dECM	Wet tissue adhesion: 151.40 ± 1.50 kPa	Deadly porcine subclavian artery hemorrhage: 32.67 ± 2.49 s. Porcine heart hemorrhage: within 1 min.	[6]
rSer-TA	Disulfide-bond hydrolyzed sericin protein	Wet tissue adhesion: >0.1 MPa for tissues	Rat liver injury: within 10 s	[7]
SHCa hydrogel	methacrylate-functionalized silk fibroin and catechol-conjugated hyaluronic acid	Adhesion strength: 136.93 ± 7.40 KPa on blood-covered substrates	Rat liver injury: within 7 s. Rat heart injury: within 14 s.	[8]
CGD hydrogels	Chitosan, β-glycerophosphate and dihydrocaffeic acid	Adhesion strength: up to 32.5 kPa.	Rat liver injury: about 1 min.	[9]
Gallol-conjugated CHI	Chitosan and gallic acid.	Long shelf-life. Adhesion strength: about 20 kPa.	Rat liver injury: <100 mg, 89.3 ± 24.5 mg for Film to Gel stored at 1 week.	[10]
MSS@CaCO <sub>3</sub>	Negatively-modified-microporous starch, calcium carbonate and protonated tranexamic acid.	Self-propelling properties, traveling against the blood flow.	Rabbit liver injury: about 50 s. Rabbit femoral artery bleeding: about 3 min.	[11]
MS@Fe4-BT	magnetic Fe <sub>3</sub> O <sub>4</sub> , microporous starch particles, bovine serum albumin and thrombin.	Magnetic field-guided delivery.	V-shaped wounds in the liver: 37 s. V-shaped wounds in the femoral artery: 152 s.	[12]
MHS	PLA	Microneedle technology.	Porcine heart injury: within seconds.	[13]
Pagoda-like multilayer microneedle patch with DCS coating	Dodecyl-modified chitosan, Poly (ethylene glycol) diacrylate and 2-hydroxy-2-methylpropiophenone	Microneedle technology.	Rabbit liver injury: about 6 s with the force about 2.66 N.	[14]
MNAs	Gelatin methacryloyl and silicate nanoplatelets.	Bioinspired hierarchical microstructures of the insects. Microneedle technology.	Rat liver injury: ~92% bleeding reduction compared with untreated injury group.	[15]
Tissue-factor targeted peptide amphiphile nanofibers	Peptide amphiphiles	Specific localization to the site of injury.	Rat liver injury: 35–59% bleeding reduction compared to controls.	[16]
Platelet-mimetic plateletsome	Liposomes and platelet membranes.	Long circulation like liposomes and wound targeting like platelets.	Rat tail injury: 61.4% and 52.2% reduction in the bleeding time compared with Lip and PV groups.	[17]
HAPPI	HA, collagen-binding peptide and von Willebrand factor-binding peptide.	Selective binding to activated platelets.	Rat tail vein laceration: reduction of >97% in both bleeding time and blood loss.	[18]
LIMB	Polyacrylamide, chitosan, gelatin methacrylate, N-(3-Dimethylaminopropyl)-N'-ethylcarbodiimide, N-hydroxysuccin-imide.	Microporous structure with functional liquids infused.	Rat liver injury: about 120 s. Pig liver incision: 17.1 mL blood loss.	[19]
DBAH	Chitosan grafted with methacrylate, dopamine, N-hydroxymethyl acrylamide.	Imitating the two key adhesive components: PIA and Dopa.	Rat liver injury: within 30 s. Rat heart injury: within 1 min.	[20]
TAPE/TB	tannic acid, poly (ethylene glycol), poly (d,l-lactide-co-glycolide)-b-poly (ethylene glycol)-b-poly (d,l-lactide-co-glycolide) triblock copolymer.	Intrinsic hemostasis inspired, forming biomimetic clot.	Rat liver injury: 16 s. Rat tail amputation: 20 s.	[21]
SSAD	skin secretion of <i>Andrias davidianus</i>	Quick wetting and achieving adhesion by SSAD ptiotens.	Rat liver injury: 28.80 ± 6.76 s. Rat tail amputation: 46.00 ± 8.72 s.	[22]

(C–CHI)/tannic acid (TA)/silk fibroin (SF) (C-CTS) hydrogel. The abundant phenolic hydroxyl groups, dynamic redox balance of phenol quinone and rapid removal of interfacial water enabled the materials to achieve a strong wet tissue adhesion pressure of 151.40 ± 1.50 kPa. The abundance of benzene rings in TA molecules and side chains of C–CHI makes the hydrogel interface hydrophobic, while hydrophilic groups are involved in removing the bound aqueous layer on the surface. Liu et al. [7] coassembled disulfide bond-hydrolyzed hydrophobic natural sericin protein and tannic acid to form a self-hydrophobic adhesive. The exposed hydrophobic amino acids repelled interfacial water and formed stable cross-links between the adhesive and the substrate. The material achieved a stable underwater adhesion to wet tissue above 0.1 MPa. Compared with conventional adhesives with Dopa, materials based on amyloid aggregates, hydrophobic components and adhesive groups are more promising in biomedicine and can be biodegradable in the human body. Lu et al. [8] further focused on the influence of a highly dynamic fluid environment on adhesion at the wound site, and they constructed an adhesive hydrogel (named SHCa) based on cyanoacrylate functionalized silk fibroin and catechol-conjugated hyaluronic acid. The silk fibroin-vinyl double bond chemical cross-linked network in the hydrogel

limited the catechol-Ca<sup>2+</sup> coordination bond strength, which resulted in rapid in situ gelation, high mechanical strength and cohesion. The hydrogel showed excellent wet adhesion strength (e.g., 132.27 ± 5.52 kPa for heart) on all blood-stained tissues (Fig. 2F).

Several studies have considered the use and storage of hemostatic materials in practical applications. Since the hydrogel needs to be positioned at the wound site in an environment close to human body temperature, Liu et al. [9] introduced dihydrocaffeic acid (DHCA) with catechol group into a chitosan solution and to prepare a thermosensitized hydrogel system. DHCA has a structure similar that of β-glycerophospholipid and promotes rapid in situ gelation of chitosan solution at physiological temperature (37 °C) and enhances bioadhesion through physical/noncovalent mechanisms. The material has an adhesion strength of up to 32.5 kPa. In response to the problem that hemostatic materials with modified polyphenol structures are prone to spontaneous oxidation and are difficult to be stored for a long time, Ju et al. [10] studied the use of gallic acid-conjugated chitosan hemostatic film to minimize spontaneous oxidation in a wet environments and maintain adhesion and hemostatic ability within 3 months. This hemostatic film transformed into an injectable hydrogel at physiological pH, effectively

## Positioning the material on the wound site

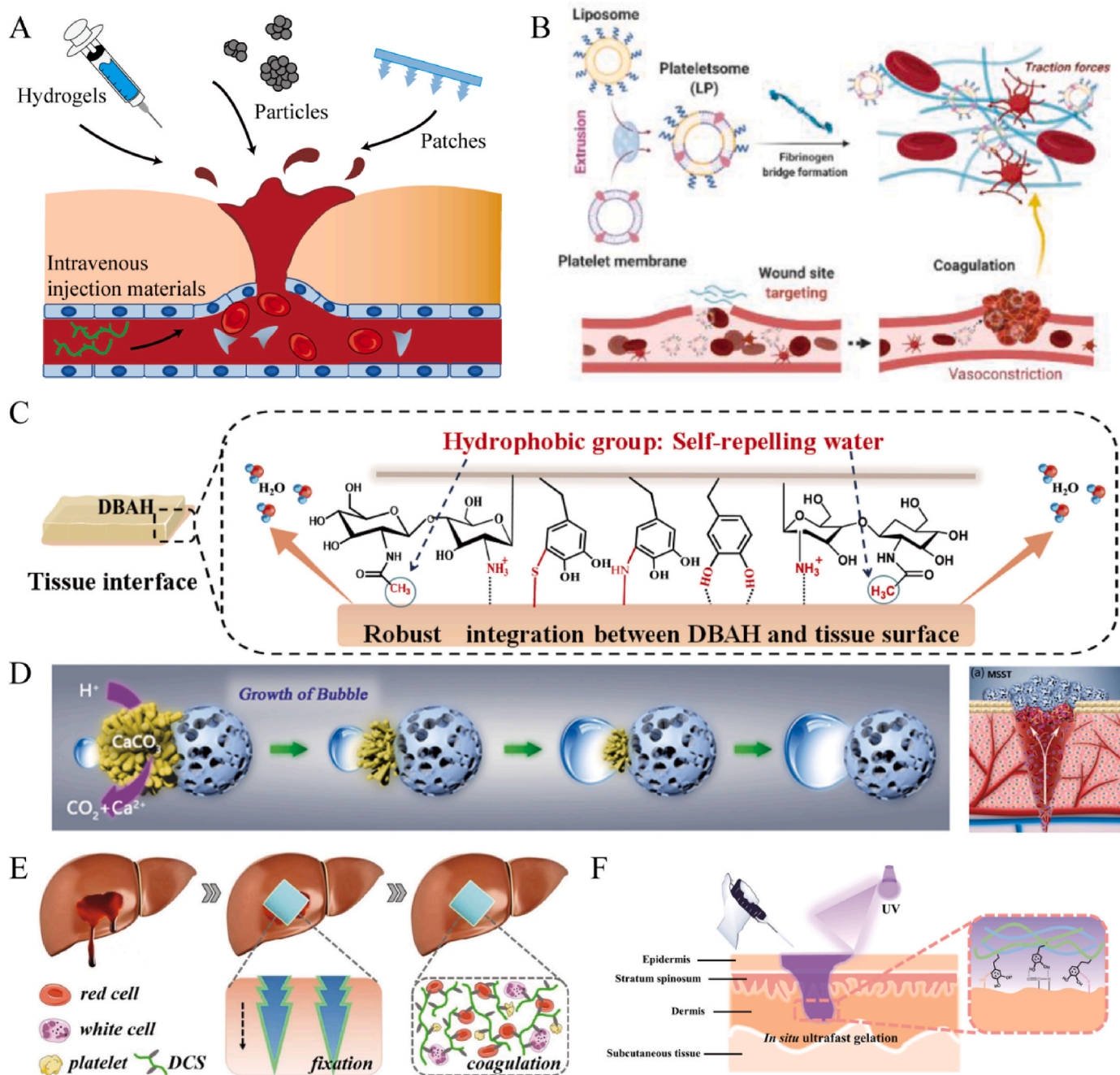


**Fig. 2.** Schematic and examples of hemostatic materials' improvement and effect on wound positioning. (A) Schematic of wound bleeding and the hemostatic materials used, including injectable hydrogels, particles, microneedle patches, intravenous targeted materials, etc. (B) Plateletsomes, hybrid nanovesicles by fusing platelet membranes and lipid membranes, target injured vascular for hemostasis. Reproduced with permission. Copyright 2022, Elsevier. (C) DBAH hydrogel achieves strong underwater adhesion base on the self-repelling water function of CS-MA. Reproduced under the terms of the CC BY Creative Commons Attribution 4.0 International License. Copyright 2020, published by Elsevier. (D) Bubble growth over the MSST Janus particle during self-propelling motion and schematic of hemostatic process. Reproduced with permission. Copyright 2020, Wiley-VCH. (E) Schematic of bioinspired pagoda-like microneedle patch for the treatment of liver bleeding hemorrhage. Reproduced with permission. Copyright 2021, Elsevier. (F) Schematic of wet adhesion mechanisms of SHCa, the catechol groups in the hydrogel network had strong binding affinity with nucleophiles of proteins. Reprinted with permission from Biomacromolecules. Copyright 2023 American Chemical Society.

stopping both internal and external bleeding.

During use, in situ gelation of the hydrogel precursor solution must be accelerated in situ gel to ensure its rapid formation at the wound site. Crosslinking based on ultraviolet light or chemical action may cause additional surgical operations and safety problems. The transformation of sols to gels at human body temperature seems to be the most

promising method. In addition, hydrogels with high adhesion performance will avoid adhesion to other tissues in the body, so it is necessary to control the amount of hydrogel or combine it with other materials to form an external antiadhesion membrane structure during use.

## 2.2. Self-pumping and magnetic field driving

Hemostatic materials in the form of particles, such as zeolite, kaolin, or microporous starch, are particularly suited for hemostasis of complex wounds, but in deep wounds affected by continuous intense bleeding, microparticle preparations are easily dispersed by blood flow and cannot exert a hemostatic effect. Investigators are actively constructing materials that can reverse blood flow into the wound and rapidly concentrate at the bleeding site through a specific driving mode.

Baulis et al. [89] first reported self-propelled microparticles consisting of carbonate and tranexamic acid that were actively transported through blood. Furthermore, based on the two-sided heterostructure of Janus particles, Li et al. [11] combined calcium carbonate with negatively modified microporous starch to prepare a self-propelling hemostatic material. By loading with protonated tranexamic acid or thrombin, these particles allow rapid control of perforations and irregular wound bleeding. In the blood, CO<sub>2</sub> is generated at the particle tail end and serves as the driving force for delivery to the bleeding site (Fig. 2D). However, if the gas is depleted before the particles reach the target location, the hemostatic particles undergo uncontrolled floating with the blood. To accurately locate the bleeding site and provide a sustained driving force, Shi et al. [12] built an intelligent microplatform, MS@Fe<sub>4</sub>-BT, for targeted hemostasis by taking advantage of the magnetic properties of Fe<sub>3</sub>O<sub>4</sub>. Bovine serum protein (BSA), a thrombin loading medium, was precisely delivered to the wound site under the guidance of magnetic field to achieve hemostasis. The constant guidance of the magnetic field concentrates these particles on deep and narrow wounds, as well as to cope with noncompressible bleeding.

Hemostatic particles have advantages in the treatment of noncompressible bleeding wounds and can effectively block the ruptured blood vessels and achieve precise treatment after magnetic field guidance. In practical applications, if the transport path of the hemostatic particles is long, it is necessary to consider whether the loss of the shed particles will affect the hemostatic effect and whether it will cause unnecessary thrombi to enter the bloodstream.

## 2.3. Mechanical interlocking

Several researchers have modified the surface microstructures of hemostatic materials and used microneedle arrays to achieve mechanical interlocking between the materials and the skin tissue to form stable adhesions without additional pressure. The microneedle array can increase the contact area between the microneedle array and the tissues, and the adhesion effect is less affected by the environment, so it causes no damage to the contacting tissues.

Yokoyama et al. [13] prepared a microneedle hemostatic sheet (MHS) for use with local hemostasis of organs and large vessels during trauma or surgery. The experiment also verified the rapid hemostasis of the MHS with a puncture of the pig left ventricular wall, and the MHS was used as a non-slip stent for gauze compression surgery. Zhang et al. [14] prepared bioinspired pagoda-shaped microneedle patches. The microneedle structure was similar to an insect foot or mouthpiece and was firmly bound to the tissue through multiple physical interlocking layers, which were not affected by massive hemorrhages. The patch was coated with dodecyl chitosan (DCS) to anchor blood cells and achieve rapid hemostasis (Fig. 2E). Haghniaz et al. [15] developed a microneedle array (MNA) with GelMA combined with silicate nanosheets to demonstrate adhesion at the wound site through the adhesive ability of gelatin and the mechanical interlocking of microneedles.

It is worth mentioning that the microneedles interacted with tissue to expand the surface area of the adsorbed platelets and promote hemostasis. In future studies, the microneedle structure could be loaded with prorepair components, growth factors or other drugs to achieve further synergies for hemostasis and wound healing.

## 2.4. Specific targeting

For internal bleeding that occurs in the body, without surface wounds or dissemination, the traditional methods of hemostasis are no longer applicable. Extensive treatment involves oral/intravenous tranexamic acid, but it usually affects only at the early stage of blood loss and there is a risk of deep vein thrombosis. Mechanically assisted interventions, such as endovascular balloon occlusion, require additional equipment and are associated with greater risks.

Hemostatic materials that are injected intravenously into the internal circulation system need to specifically target changes in factor levels in the bleeding portion to achieve control of internal bleeding. Some studies were designed to accelerate the eventual formation of eventual fibrin clots by targeting the delivery of a clotting cascade or fibrinogen through intravascular delivery. Klein et al. [16] have prepared a series of TF-targeted peptide amphiphilic (PA) nanofibers to specifically localize noncompressible hemorrhage *in vivo*. A therapeutic agent was delivered to the site of TF exposure after injury, enabling a simple intravascular route for systemic administration.

Another research direction was based on the role of platelets during the bleeding. Clinical transfusion of concentrated platelets is a viable treatment method, but is limited by a short shelf life, lack of donors and immune problems. There have been multiple studies on platelet biomimetics/substitutes. Wang et al. [17] started from the hemostatic characteristics of platelets combined with fibrin to form thrombosis, and the liposomes hybridized with the platelet membrane to form a nano-hemostatic platform. This biomimetic material retains the natural structure of platelets on the surface and targets injured blood vessels to control massive bleeding (Fig. 2B). Gao et al. [18] prepared a hemostatic agents via polymer peptide interfusion (HAPPI), a conjugate of hyaluronic acid with collagen binding peptide and von Willebrand factor binding peptide (vWF). HAPPI targets the vWF and collagen and selectively combines with activated platelets to enhance blood clot formation.

Unlike the hemostatic materials described above, intravenous hemostatic materials must provide a balance between coagulation ability and targeting accuracy. In clinical treatment, anticoagulant therapy is sometimes necessary to prevent trauma-induced coagulopathy (TIC) and prevent thrombosis formed in the hypercoagulable state of patients from blocking arteries or organs. However, intravenous hemostatic materials can easily cause local unnecessary thrombus formation during transport and application. If the target positioning is not accurate, this will lead to a decreased hemostatic effect and additional hidden dangers. In addition, targeted therapy addresses only early management of hemorrhage, and other forms of diagnosis and treatment must still be synergistic to ensure mitigate the danger of the casualty.

## 2.5. Other bio-inspired design

In addition to the catechol group design inspired by mussel adhesion, some studies have been focused on wet adhesion models from other biological sources and made biomimetic design or utilization. Inspired by the synergistic action of lipids and adhesive proteins in barnacle glue, Bao et al. [19] prepared a paste adhesive with bioadhesive microparticles mixed with hydrophobic matrix. The lipid matrix first cleaned the underlying substrate by repelling water and contaminants, and subsequently the adhesive proteins cross-linked with the substrate to form a stable and strong adhesion. In addition to mussel protein adhesion, Han et al. [20] also used cationic polysaccharide intercellular adhesin (PIA) in staphylococcal biofilms to construct a dual biomimetic strategy and synthesized a dual biomimetic adhesion hydrogel (DBAH). The large number of hydrophobic -CH<sub>3</sub> residues in the PIA-like structure of the hydrogel repelled water molecules on the wet surface, promoting the exposure and close contact of dopamine (DA) and NH<sub>3</sub><sup>+</sup> and allowing fast and strong adhesion (Fig. 2C). Inspired by the natural process of intrinsic hemostasis in the human body, Sekhar et al. [21] prepared an

insoluble water-based hemostatic powder based on liquid-liquid phase separation. Composed of TA, poly (ethylene glycol) (PEG) and poly (d, l-lactide-co-glycolide)-b-poly (ethylene glycol)-b-poly (d, l-lactide-co-glycolide) triblock copolymer (TB), the condensates can rapidly formed biomimetic clots in wounds, resulting in effective hemostasis through strong adhesion and rapid surface gelation. The additional advantage of the biomimetic design of the material is that it does not rely on the human coagulation mechanism and therefore provides effective hemostasis support for people with coagulopathy. Zhang et al. [22] extracted hemostatic particle from the skin secretion of *Andrias davidianus* (SSAD), this particle can be wetted by blood or gelled by PBS/saliva in advance and adhered to the bleeding site. A variety of proteins in SSAD are related to the adhesive properties of the *Andrias davidianus* mucus.

### 3. Stability of the material structure

After reaching the wound site, hemostatic materials play an immediate role. Hemostasis occurs through two main mechanisms: (1) Activation and promotion of the human coagulation cascade by regulating the levels of multiple coagulation factors (such as FVIII and FXIII) to promote hemostasis, platelet activation, and erythrocyte aggregation. In addition, the rapid construction of fibrin at the bleeding site can also be promoted by anti-fibrinolysis, enhancing hemostatic effects. (2) Form a physical barrier at the bleeding site based on self-adhesion ability to block blood flow, and the blood is quickly absorbed through the porous structure to promote agglutination. This mechanism relies on the mechanical strength of the material, but it avoids part of the biosafety problems associated with possible coagulopathy caused by the casualty itself.

Additionally, rapid positioning at the wound site is not enough to ensure that hemostatic materials will function, and they must have sufficient mechanical strength to continuously resist the effects of internal (blood flow) and external (motion or impact) pressure. Otherwise, structural disruption of the hemostatic material usually leads to hemostasis failure. For superficial wounds or surgical sites, suturing is generally necessary to avoid secondary injury and infection. Traditional medical suture methods require sutures or sealants, which are time-consuming and leave scars in the wound. Materials with good mechanical strengths and stabilities can replace the surgical threads to

close the wound, avoid the problems caused by surgical thread degradation and reduce the workload of health care staff (Fig. 3 and Table 2).

The ability of a material to maintain a wound is measured by its interactions with the adhesive substrate and also with the cohesion and toughness of the material itself [90]. To prevent high-pressure blood from breaking through the barrier of hemostatic materials, it is necessary to strengthen the mechanical strength of the materials and maintain their integrity during hemostasis (Fig. 3A). The burst pressure strength indicates the ability of a material to resist wound blood pressure [29]. The maximum water pressure strength of the material is measured to determine its ability to the tissue. In general, a hemostatic material is subjected to a pressure of at least 120 mmHg, the human systolic blood pressure threshold.

#### 3.1. Increasing the crosslinking structure

The strategies for preparing useful hydrogels include the construction of additional crosslinks, increasing polymer chain entanglements, and increasing the dissipation energy. Wang et al. [23] modified highly branched chain aminoethyl gelatin with catechol and formed a double crosslinked hydrogel by covalent bonding with horseradish peroxidase (HRP)/hydrogen peroxide ( $H_2O_2$ ) through instant curing catechol and  $Fe^{3+}$  chelation. The material achieved effective carotid artery closure and rapid hemostasis at the sites of liver incisions and penetrated cardiac wounds within 10 s. The wet tissue adhesion force reached  $115.0 \pm 13.1$  kPa and the burst pressure was  $245.0 \pm 33.8$  mm Hg. Peng et al. [24] prepared polyethylene imine/polyacrylic acid/quaternary ammonium chitosan (PEI/PAA/QCS) self-gelling powders. The powder first rapidly absorbed blood within 4 s to enrich the coagulation factors, and formed a physical cross-linked hydrogel to further increase adhesion. The strong physical barrier resulting from water absorption by material resisted the burst pressure of approximately 240 mm Hg. Biological ionic liquids (BILs) are structural precursor of the phospholipid layer of cell membrane. After physical cross-linking with gelation (GEL) or poly (ethylene glycol) (PEG), the improved electrostatic interactions prevented inter-chain sliding and enhanced the mechanical properties of the material. Krishnados et al. [25] prepared two kinds of hemostatic adhesives formed by coupling biological ionic liquids. After adjusting the BIL concentration, the bursting pressures reached  $101.74 \pm 2.12$  kPa (GEL) and  $69.42 \pm 1.59$  kPa (PEG). Huang et al. [26] reported multifunctional

**Table 2**  
Summary of measures to improve the stability of the material structure.

Name	Material Components	Improved properties	Main models and hemostasis time	Reference
CAGA	Catechol-modified aminoethyl gelatin, horseradish peroxidase, hydrogen peroxide, $Fe^{3+}$ .	Burst pressure: $100.7 \pm 5.2$ mm Hg after 10 s and $245.0 \pm 33.8$ mm Hg after 10 min.	Rat liver injury: several seconds with blood loss <0.05 g.	[23]
PEI/PAA/QCS powder	Polyethyleneimine, polyacrylic acid, quaternized chitosan	Burst pressure: about 240 mm Hg.	Rat liver/heart/femoral artery injury: in 10 s.	[24]
BioGel/BioPEG	Choline-based bioionic liquid, polyethylene glycol diacrylate, gelatin methacryloyl.	Burst pressure: $101.74 \pm 2.12$ kPa (GEL) and $69.42 \pm 1.59$ kPa (PEG).	Rat tail injury: in 2 min.	[25]
MFf	Aldehyde-functionalized chitosan, crosslinked poly (acrylic acid)	Burst pressure: 127 mm Hg and 485 mm Hg with plastic backing.	Incised epicardial surface of a rabbit liver: 5 s with gentle pressing.	[26]
PAAm-TA-KA hydrogels	Polyacrylamide, tannic acid, kaolin.	Burst pressure: 0.09 MPa.	Rat femoral artery: 24–31 s.	[27]
PLGA/PEG/silica composite sealants	Poly (lactic-co-glycolic acid), polyethylene glycol, silica particles.	Burst pressure: about 160 mm Hg.	Big liver injury: stopped bleeding except for a large vessel in 10 min.	[28]
GelMA/HA-NB/LAP	Methacrylated gelatin, N-(2-aminoethyl)-4-(4-(hydroxymethyl)-2-methoxy-5-nitrosophenoxy) butanamide, glycosaminoglycan hyaluronic acid, phenyl-2,4,6-trimethylbenzoylphosphinate.	Burst pressure: 280 mm Hg.	Pig penetrated cardiac injury: within 10 s.	[29]
GelMA/OD/Borax hydrogel	Methacrylated gelatin, oxidized dextran, borax.	Burst pressure: 165 mm Hg.	Rat liver injury: within 30 s. Rat heart injury: within 30 s.	[30]
NOCA	N-octyl-2-cyanoacrylates	Burst pressure: 16.66 kPa.	Pig liver injury: within 5 s.	[31]
HMCS	Poly (N-isopropylacrylamide), chitosan, polyethylene terephthalate surgical mesh.	Burst pressure: 185 mm Hg.	Sheep carotid artery/lung/liver: unquantified.	[32]

## Stability of the material structure

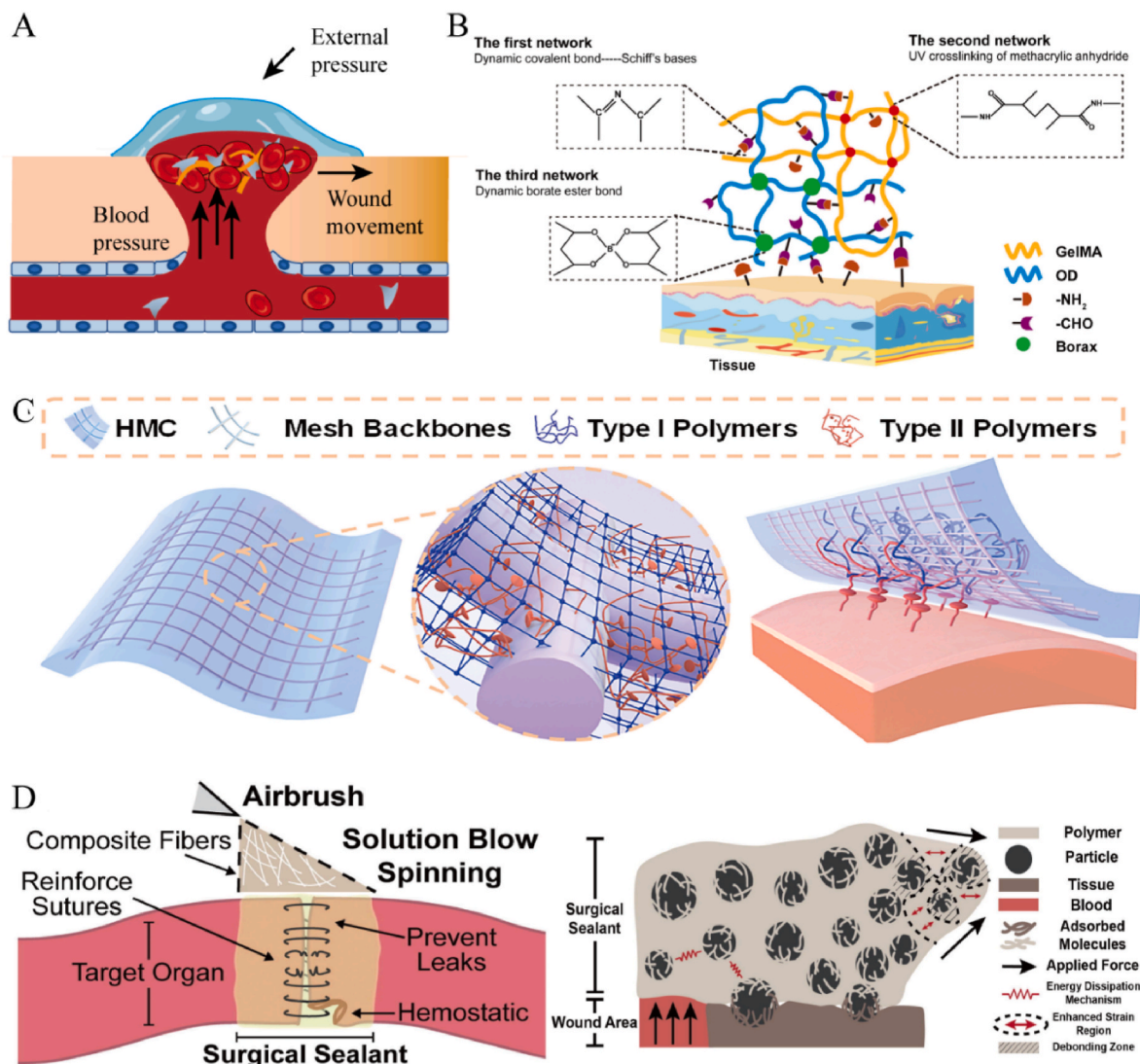


**Fig. 3.** Schematic and examples of improvement and effect of the stability of material structure. (A) Schematic of the diverse interacting forces that a hemostatic material must withstand when applied to a wound. (B) GelMA/OD/Borax hydrogel has a triple-network structure, including UV light-induced crosslinking, Schiff base and dynamic boric acid ester bond. Reproduced with permission. Copyright 2021, Elsevier. (C) In the HMC, the hydrogel and the surgical mesh form topological entanglement. Reproduced with permission. Copyright 2021, PNAS. (D) PLGA/PEG/silica composite sealants direct deposited on target organ and the schematic of the multiple toughening and adhesion enhancing mechanisms by incorporating silica particles. Reproduced with permission. Copyright 2019, Elsevier.

films (MFFs) with interpenetrating network structures based on self-crosslinked aldehyde-functionalized chitosan (AC) and crosslinked polyacrylic acid (PAA) further coordinated with Ag<sup>+</sup>. The synergistic design of the covalent and ionic cross-linking networks improved the toughness of the MFF, and the material was able to withstand 127 mm Hg burst pressure, and this limit increased to 485 mm Hg when combined with a plastic backing.

Notably, excessive crosslinking may lead to difficulty in degrading and removing the hydrogels and biosafety problems. The addition of crosslinking agents/raw materials also inhibits clinical translation and practical application of the hemostatic materials. We will discuss these issues in the following sections.

### 3.2. Combining nanoparticles

Some studies have added nanoparticles to polymers. The polymer-nanoparticles design enhances the interfacial adhesion energy, and increase the fracture energy of the hydrogel system by inhibiting cracks,

which improves the ability to maintain wounds. Fan et al. [27] prepared a tough polyacrylamide (PAAM)/TA/kaolinite (KA) adhesive hydrogel. The cross-linked network of TA and KA endowed the hydrogel with high strength and toughness, and the KA nanoparticles accelerated thrombosis as well as served as a physical crosslinking agent. The hydrogel absorbed considerable external work and the maximum bursting pressure was 0.09 MPa. Daristotle et al. [28] incorporated silica particles into poly (lactic-co-glycolic acid) (PLGA) -PEG polymer sealant to enhance tissue adhesion. The solution mixed with silica was sprayed directly on the wound in situ, and the intestinal burst pressure was comparable to that of cyanoacrylate glue (160 mm Hg) (Fig. 3D).

Additionally, targeted mineralization of metal nanoparticles has been utilized to enhance the overall mechanical properties of materials [91]. By employing a bioinspired approach to targeted mineralization, organic-inorganic composites were synthesized as integrated entities rather than simply being loaded or mixed together. Consequently, traditional defects or voids were avoided, while combined application of organic-inorganic composites in multiple fields, such as in tissue

engineering, wearable electronics, and drug delivery, can be achieved.

### 3.3. Photoinitiated polymerization

Light-curing crosslinking can accelerate the *in-situ* gelation of hydrogels and increase their mechanical strengths. Hong et al. [29] designed methacrylated gelatin/glycosaminoglycan hyaluronate acid linked it with N-(2-aminoethyl)-4-(4-(hydroxymethyl)-2-methoxy-5-nitrosophenoxy) butanamide/lithium phenyl-2,4,6-trimethylbenzoylphosphine (GelMA/HA-NB/LAP) gel that mimicked the composition of the extracellular matrix. The material was cross-linked by ultraviolet light to form a dual structure of GelMA and Schiff base cross-linked structure. The experimental results showed that the material could withstand blood pressures up to 290 mm Hg, sealed the porcine heart puncture wound within 20 s and quickly stopped bleeding. Chen et al. [30] used GelMA/oxidized dextran (OD)/borax to construct a hydrogel network with a triple cross-linked structure formed by photoinitiated polymerization, Schiff base bond and dynamic borate bond, which greatly enhanced the overall mechanical properties (Fig. 3B). When the hydrogel failed, the bursting pressure had reached  $165.53 \pm 11.77$  mm Hg and the wound closure strength was  $60.05 \pm 16.18$  kPa. It is worth noting that although the authors stated that short-term UV radiation did not cause damage to the cells at the wound site, additional light applied during surgery may affect further manipulation and stability.

### 3.4. Other reinforcement methods

Moreover, other reinforcement methods can also be used to increase the bursting strength of the hemostatic material itself. Zhang et al. [31] used laparoscopy to perform *in situ* electrospinning of N-octyl-2-cyanoacrylate (NOCA) during minimally invasive surgery to achieve rapid hemostasis through precise deposition. NOCA could withstand a pressure of 16.66 kPa, which was greater than normal blood pressure. The advantage of *in situ* deposition is that it avoids the problem of poor adhesion caused by the inability of electrospun membranes prepared *in vitro* to fit the wound tissue. Gao et al. [32] developed a series of hydrogel-mesh composites (HMCS) in which surgical mesh was soaked with hydrogel precursors and cured to form macroscopic topological entanglements. When adhering to tissue and subjected to blood flow pressure, the mesh acted as a skeleton to disperse the stress across a large area of tissue, the material is able to withstand a pressure of 185 mm Hg (Fig. 3C).

With intractable bleeding emergencies, hemostatic materials must quickly adhere to and seal the bleeding site, which requires shortening the preparation time of hemostatic materials, such as the time required for *in situ* injection and gelation time of the hydrogel. For materials that have been pre-cut or prepared, it is often difficult to cope with complex situations quickly. In other words, it is necessary to further improve the interaction between the performance of the material and its practical application to further develop the hemostatic materials for emergency applications.

## 4. Easy removal or degradation after hemostasis

When the emergency treatments of open injuries and extensive surface injuries is finished, it is necessary to remove hemostatic materials around the wound as much as possible, since further surgery and other treatments may be needed after hemostasis. As mentioned before, compression with gauze or tourniquet is the simplest and most convenient way to stop bleeding during emergency rescue, but these materials have adverse effects: gauze absorbs blood and forms attached blood clots, which can easily cause secondary injury when peeled off [92]. Similarly, after complete hemostasis, the residual hemostatic material sometimes acts as a foreign body to trigger inflammation during subsequent wound healing. Therefore, consideration should be given to

removing the remaining hemostatic material from the wound as much as possible after hemostasis. Simple detachment or rapid degradation is the main research goal (Fig. 4 and Table 3).

### 4.1. Easy and rapid detachment

Strong adhesion and removal of hemostatic materials seem to occur at opposite ends of the treatment spectrum, since the high dissipation energy or multiple bonding interactions cause the material to bind more closely to the wound tissue. Easy and rapid detachment avoids the risk of secondary bleeding after hemorrhage is controlled, and additional treatment may be needed (Fig. 4A).

#### 4.1.1. Removal of bonding interactions

Several researchers have sought to achieve multiple adhesion-peeling effects by specifically and rapidly cutting chemical bonds or chain structures to remove materials, and controlling the reversibility of interfacial bonding. Pan et al. [33] prepared N-hydroxysuccinimide (NHS) ester-activated carboxymethyl cellulose (CMC-NHS) aerogel in which a semistable NHS ester reacted with primary amine groups on the wound surface to generate stable adhesion. After complete hydration with PBS, the aerogel maintained its morphology and structural strength, while the CMC at the interface dissolved, resulting in easy removal of the material from the wound (Fig. 4C). The CMC remaining in the wound was also be further broken down by glycosidases or macrophages. Yang et al. [34] developed a multifunctional dynamic Schiff base network hydrogel incorporating a melanin-inspired polydopamine@polypyrrole (PDA@PPy) nanocomposite. Based on the dynamic redox response of disulfide bonds inspired by the dissociation of the tertiary spatial structures of polypeptide chains, hydrogels can be rapidly and painlessly removed on demand by the addition of dithiothreitol under mild conditions. The hemostatic patch APTF developed by Zheng et al. [35] demonstrated robust tissue adhesion through the chemical coupling of NHS to alginate molecules and the incorporation of TA. The synergistic effect of TA/Fe<sup>3+</sup> resulted in better cohesion and excellent hemostatic effects. After a safe dose of 0.1 M urea, the hydrogen bonds between APTF and the tissue were cleaved to achieve controlled separation.

#### 4.1.2. Dealing with reversible coordination bonds

The coordination complexes of metal ions and organic compounds can be used to construct a dynamic cross-linking network and facilitate the gelation process, and these bonds can also be exploited to break or further strengthen the hydrogel structure. Cao et al. [36] used the coordination bond between Fe<sup>3+</sup> and carboxyl group in carboxymethyl chitosan (CMCh) to construct a dynamic cross-linked network hydrogel. After the hydrogel was treated with SO<sub>4</sub><sup>2-</sup> solution, a large number of cross-links formed between the amino groups of CMCh and SO<sub>4</sub><sup>2-</sup> and induced phase separation of the hydrogel, so it was easily removed from the wound site without leaving a residue. The peeling tension of the material was 34–39 times lower than those of commercially available hemostatic agents. Liang et al. [37] constructed a double dynamic bonded hydrogel with Fe<sup>3+</sup>, protocatechual (PA), and quaternary ammonium chitosan (QCS). Deferoxamine mesylate (DFO), a medical Fe<sup>3+</sup> chelator, can remove the catechol-Fe<sup>3+</sup> coordination bond and help remove the hydrogel from the wound. The material can be used as a wound adhesive to help change dressings as needed and avoid secondary damage to the wound. The hydrogen-bonded hydrogel PAAcVI proposed by Wang et al. [38] was prepared from acrylic acid and (AAc) and 1-vinylimidazole (VI) in DMSO followed by solvent exchange with water. Since Zn<sup>2+</sup> exhibits good reactivity with imidazole, the material can be reduced by the addition of Zn<sup>2+</sup> solution to form complexes with imidazole, the hydrogel was degraded by the addition of Zn<sup>2+</sup> to form complexes with imidazole, and the tissue can be painlessly peeled off.

**Table 3**  
Summary of measures to improve on-demand detachment of hemostatic materials.

Name	Material Components	Improved properties	Main models and hemostasis time	Reference
CMC-NHS aerogel	Citric acid, N-hydroxysuccinimide, carboxymethyl cellulose.	Easily removed when fully hydrated.	Rat liver injury: 25.1 ± 10.9 mg blood loss.	[33]
HA-CYS/PFA/PDA@PPy Hydrogels.	cystamine-modified hyaluronic acid, benzaldehyde-functionalized poly (ethylene glycol)-co-poly (glycerol sebacate), and polydopamine@ polypyrrole nanocomposite.	Rapid painless on-demand removal by dithiothreitol.	–	[34]
APTF	Poly (ethylene glycol) diacrylate, N-hydroxysuccinimide, alginate, tannic acid, Fe <sup>3+</sup> .	On-demand removal with 0.1 M urea	Rat liver injury: 2.77 ± 1.74 mg blood loss.	[35]
CMCh hydrogel	Carboxymethyl chitosan, Fe <sup>3+</sup> /Al <sup>3+</sup> .	Swiftly detached with SO <sub>4</sub> <sup>2-</sup> .	–	[36]
Dual-dynamic-bond crosslinked hydrogel	Fe, protocatechualdehyde, quaternized chitosan.	On-demand removal with deferoxamine mesylate or acid solution.	Rat liver injury: 102 mg.	[37]
PAAcVI hydrogel	Acrylic acid, 1-vinylimidazole (VI).	Zn <sup>2+</sup> -ion-mediated on-demand debonding.	Rat liver injury: within 1 min.	[38]
w-TAGel	N-isopropylacrylamide, acrylamide, gelatin methacrylate, urushiol.	Water-driven noninvasively detachment at 25 °C	Rat liver injury: within 30 s.	[39]
Chitosan–Catechol–pNIPAM	Chitosan, Catechol, poly (N-isopropyl acrylamide), Fe <sub>3</sub> O <sub>4</sub> NPs.	Controllable thermo-responsive adhesion/detachment.	Rat venipuncture with needle: 2 µL at 30 s.	[40]
LIMBs	Polyacrylamide, chitosan, gelatin methacrylate, N-(3-Dimethylaminopropyl)-N'-ethylcarbodiimide, N-hydroxysuccin-imide.	On-demand removal by saline (disable physical interactions), acetic acid and lysozyme (when chemical bonds form)	Rat liver injury: about 120 s.	[19]
A bioadhesive capable of instant tough adhesion and triggerable benign detachment	polyvinyl alcohol, poly (acrylic acid), N-hydroxysuccinimide.	Triggerable detachment by sodium bicarbonate and glutathione at different adhesion times.	Pig liver incision: 17.1 mL blood loss.	[41]
Modified cotton gauze	1,2benzenediol-3-(7,9,13-pentadecatrienyl), cotton gauze.	Dam-shaped barriers prohibit blood from seepage and prevent rebleeding.	–	[42]
Nonwetting nanostructured hemostatic material	Beeswax, carbon nanofibers, kaolin microparticles, gauze.	Micro/nanoscale point-to-point contact with the clot, low clot peeling tension.	Rat femoral artery injury: 34 s. Pig femoral artery injury: about 0.80 g. Rat back bleeding: 1.8 ± 1.2 mg.	[43]
PDMA-b-PFOEMA	Poly (N,N-dimethylaminoethylmethacrylate), poly (1H,1H,2H,2H-heptadecafluorodecyl acrylate).	Temperature triggered detachment.	Rat tail amputation: unquantified.	[44]
Injectable hemostatic PEG-based hydrogel w	4-arm PEG (thioester)-CHO, poly (ethylene imine), adipic dihydrazide.	On-demand dissolved by L-cysteine methyl ester.	Rat liver laceration: within 15 s. Rat liver resection: within 30 s.	[45]
SS	Tetra-PEG-NH <sub>2</sub> , tetra-armed poly (ethylene glycol) succinimidyl succinate.	Controllable dissolution with cysteamine within 5 min.	Rabbit liver injury: within 30 s. Pig spleen injury: 5 min.	[46]
DNGel	Methacrylated gelatin, dopamine N-isopropylacrylamide, Fe <sup>3+</sup> .	On-demand dissolved by acetic acid.	Rat liver injury: 0.12 ± 0.03 mg.	[47]
PBO hydrogels	Polyvinyl alcohol, borax, oligomeric procyanidin.	On-demand removed based on fast degradation in water.	Rat liver injury: 20 s. Rat leg artery injury: 49 s.	[48]
Sprayable polymer-based foam	Hydrophobically modified chitosan	Sustains foam structure and hemostasis for up to 60 min without compression.	Pig liver injury: decreased 90% blood loss compared with controls.	[49]
Hemostatic foams with improved rheology.	Hydrophobically modified chitosan, hydrophobically modified alginate, acetic acid, sodium bicarbonate.	More robust barrier to blood discharge	Pig liver injury: unquantified but superior to the former.3	[50]

#### 4.1.3. Temperature-triggered detachment

On-demand separation and fitting of hemostatic materials based on temperature triggers is an ideal and simple method that avoids the harm caused by chemical treatment of the human body. A temperature-triggered phase transition ability of N-isopropyl acrylamide (NIPAM) makes it a potential material. Huang et al. [39] prepared water-driven detachable wet tissue adhesive hydrogel (w-TAGel). The physical cross-linking site formed by the hydrophobic aggregation of isopropyl groups was interrupted by water treatment at 25 °C, resulting in volume expansion of Poly (NIPAM-co-AAm-co-GelMA-co-Urushiol) (PNAGU), reducing interfacial bonding, and rapid separation of the hydrogel. Xu et al. [40] prepared chitosan-catechol-pNIPAM hydrogels that exhibited a reversible sol-gel transition at a critical transition temperature of approximately 35 °C. In particular, the addition of Fe<sub>3</sub>O<sub>4</sub> NPs to the hydrogel that was then coated on the PVA hydrogel substrate enabled

remote controlled thermally responsive adhesion/separation with the skin under NIR light irradiation.

#### 4.1.4. Detachment for different periods

In the study by Bao et al. [19], the unstructured design of a liquid-infused microstructured bioadhesive (LIMB) supported different removal methods: saline was used to wet the material within 2 min; a low concentration of acetic acid solution was then used to degrade the bonding interactions formed at the interface. Chen et al. [41] used a highly hygroscopic polyacrylic acid (PAA) network to remove the surface water and prepared PVA and PAA wet adhesion hydrogels with interpenetrating networks. The relative contributions of physical (hydrogen bonding) and covalent (amide bonding) cross-links at different adhesion times were further investigated. The authors also proposed biocompatible separation of the material by sodium

## On-demand removal

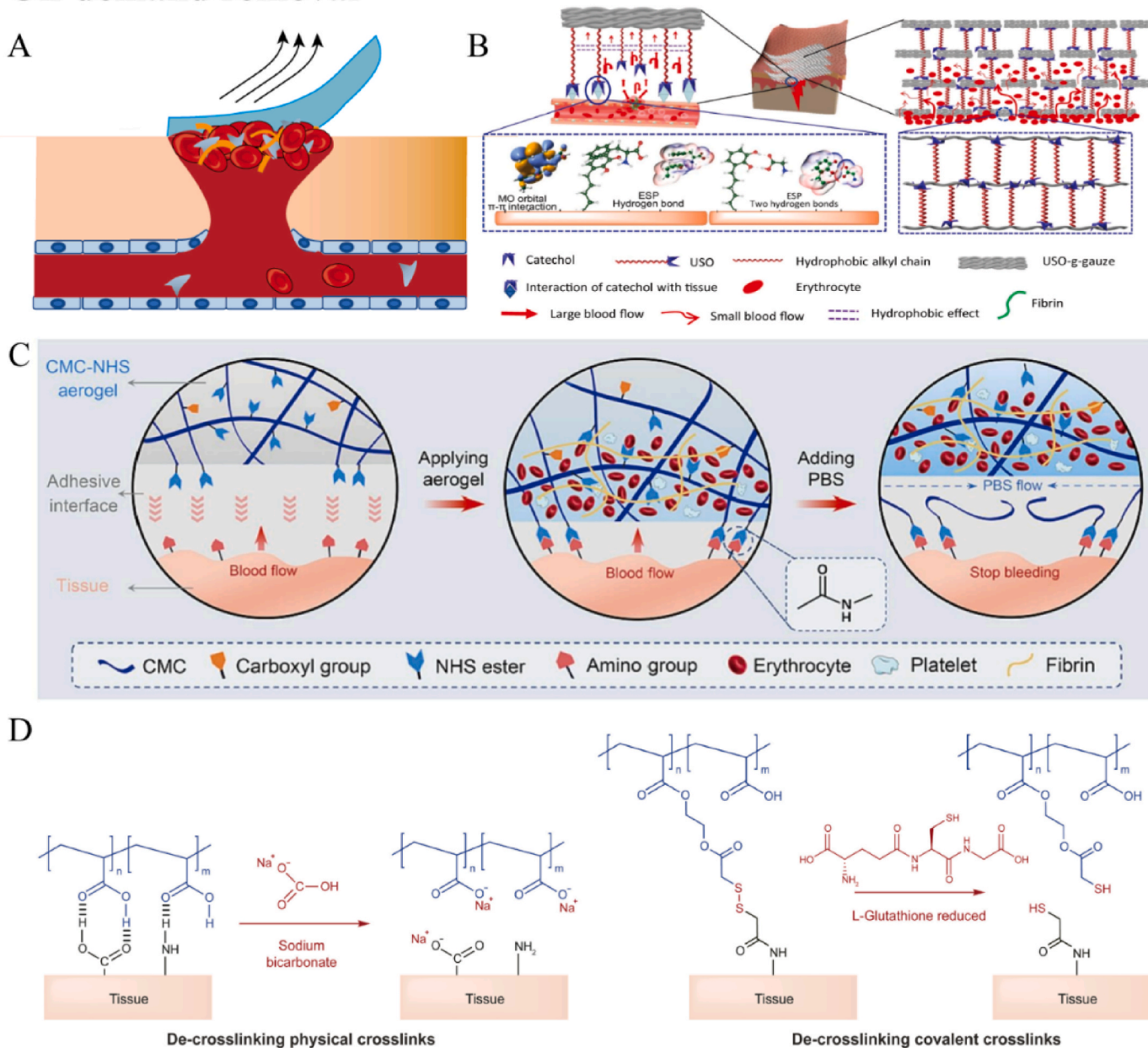


**Fig. 4.** Schematic and examples of hemostatic materials' improvement and effect on on-demand removal. (A) Schematic of detachment of hemostatic materials from wound. (B) USO-g-gauze forms a dam-shaped barriers to aggregating RBCs to form clot, reducing damage to blood clots during removal. Reproduced under the terms of the CC BY Creative Commons Attribution 4.0 International License. Copyright 2022, published by Springer Nature. (C) When CMC-NHS aerogel adhered to the wound, the CMC at adhesive interface can be completely hydrated by PBS and the aerogel can be easily removed. Reproduced with permission. Copyright 2023, Elsevier. (D) Two different triggerable detachment mechanisms of the instant, tough, and triggerably detachable bioadhesive, removing physical and covalent crosslinks. Reproduced with permission. Copyright 2020, PNAS.

bicarbonate (SBC) and glutathione (GSH) over a wide time span (Fig. 4D). In both studies, the authors focused on the removal of hemostatic materials at different time scales and responded to the need for effective repositioning from a designated site within minutes and removal from a designated site after weeks; this provided more flexibility in the use of hemostatic materials.

### 4.2. Reduce interaction with blood clots

Due to the strong hydrophilicity of traditional gauze, bandages and other hemostatic materials, the blood clots are closely adhered to the material, which can easily tear blood clots and cause secondary bleeding

during peeling. Several literature have investigated the improvement of adhesion between materials and blood clots. Reduced adhesion facilitates easier removal of the material from the wound, while safeguarding the blood clot against tearing and subsequent bleeding. He et al. [42] modified traditional cotton gauze by grafting long-chain alkyl groups and the catechol derivative 1,2-benzenediol-3-(7,9,13-pentadecatrienyl) (USO). This modified gauze constructed many dam-shaped barriers at the contact surface and adjacent fibers, rapidly aggregated red blood cells to form blood clots, and prevented blood from covering the gauze and oozing from the junction (Fig. 4B). The aggregated red cell clots were largely retained at the time of material removal and therefore did not contribute to rebleeding. Blood contracts after coagulation, and

this property can be used to optimize the contact structure of the material and the blood-clot interface to achieve the minimum stripping. Li et al. [43] prepared a non-wettable nanostructured fiber material with hydrophobic beeswax immobilized carbon nanofibers (CNFs) and further added kaolin microparticles to increase the coagulation energy. Microporous bubbles were formed between the nanofiber structure and the clot, which enabled micro/nano point-to-point contact between the material and the clot, and the material was easily removed when the blood clot formed and contracted. Li et al. [44] developed an antibacterial/hemostatic material based on poly (N, N-dimethylamino ethyl methacrylate) -*b*-poly (1H, 1H, 2H, 2H-heptafluoro-decyl acrylate) (PDMA-*b*-PFOEMA) block copolymer. The quaternary ammonium copolymer coating was susceptible to temperature triggering. It exhibited a synergistic antibacterial effect at room temperature and converted to a superhydrophobic interface near body temperature to repel blood. The design strategy for temperature regulation allowed separation of the coating from the blood clot and avoided tearing of the wound when removed.

#### 4.3. Rapid self-degradation

Apart from the slow degradation and absorption of materials over a long time in the body, if after hemostasis, the material could quickly degrade the components that are not harmful to the human body with the help of a simple reaction, this process would aid subsequent treatment. Shi et al. [45] first prepared 4-armed PEG (thioester)–CHO containing thioester bonds and aldehyde groups, and then formed a hydrogel in situ via a Schiff base reaction with poly (ethyleneimine) (PEI) and dihydrazide adipate (ADH). The hydrogel dissolved in a solution of L-cysteine methyl ester (CME) solution on demand via a thiol-thioester exchange reaction without additional treatment. The four-arm polyethylene glycol amine hydrogel prepared by Bu et al. [46] was based on ammonolysis and introduced a cyclic succinyl ester group, which enabled controlled dissolution and rapid degradation. Rapid removal of the hydrogel from both smooth skin (2 min) and irregular wounds (5 min) was achieved by soaking the swab with the alkaline drug cysteamine (CA). Hou et al. [47] also synthesized the formylated gelatin and N-isopropyl acrylamide (NIPAAm) hydrogel DNGel via a double syringe method based on the catechol-Fe<sup>3+</sup> coordination bonding. The PH response of catechol-Fe<sup>3+</sup> allowed controlled dissolution of the material in acetic acid. Although the adhesive strength of the material was extremely high (3.25 MPa), it rapidly decreased to 0.62 MPa after treatment with the acetic acid solution, at which point the material could be removed from the wound. He et al. [48] prepared a removeable PBO hydrogel with PVA, borax, and oligomeric proanthocyanidins (OPCs). The PBO was degraded in situ within 10 min by the addition of deionized water, but remained stable in the presence of saline, PBS, and blood, so it could be removed on demand after wound closure. Dowling et al. [49] prepared hydrophobic modified chitosan as a hemostatic agent in the form of liquid foam, which formed a self-supporting barrier, maintained a stable structure for 5 min and prevented liver injury and bleeding in pigs, and finally dispersed into harmless absorbable liquid. Sprayed foam hemostatic materials may be a potential form of hemostatic agents for rapid hemostasis at emergency rescue sites. Furthermore, they introduced a hydrophobic alginate modification and used a double-tube syringe for in-situ foam moulding to produce a surfactant-free foam with opposite charges, which showed substantial hemostatic effect [50].

Regardless of the improvements, on-demand removal or dissolution allows rapid relocation and painless removal of the material from the wound site, reducing the need for additional surgery by medical staff and reducing patient pain. Therefore, in practical application, removal on demand is a crucial improvement. More attention should be given to protecting blood clots at the wound site by reducing the interactions and improving the mechanical properties (especially the fracture toughness) of the clots.

## 5. Sustained action at the site of injury

When used as a surface wound dressing or as a hemostatic material for difficult to remove parts of the body, such as organs, blood vessels and tissues, it is expected that the material will play additional roles during its retention period to support further wound repair. These functions include continuous antibacterial, anti-adhesion, rapid discharge of residual biofluid from the wound, and promotion of tissue repair and wound healing (Fig. 5 and Table 4).

### 5.1. Preventing tissue adhesion

The large amount of fibrin and the proliferation of fibroblasts resulting from wound hemostasis coupled with the high adhesiveness of the hydrogel itself, increase the likelihood of unnecessary adhesion to other tissues and organs, causing patients suffer additional pain [93]. Several researchers have modified the nature of the outer interface of the hydrogels to form a physical barrier interface that prevented adhesion. Wei et al. [51] designed an injectable hydrogel based on dodecyl-modified N-carboxyethyl chitosan (DCEC) and oxidized Konjac glucomannan (OKGM), which combined the hemostatic and antibacterial properties of DCEC and the properties of OKGM to reduce inflammation at the wound site. Bleeding was effectively stopped in the liver resection model. Moreover, the physical barrier prevented postoperative adhesion and inhibited the expression of TNF- $\alpha$  and TGF- $\beta$ . Li et al. [52] prepared hybrid hydrogels consisting of oxidized hyaluronic acid, ethylene glycol chitosan, and conditioned medium (CM) from menstrual blood-derived stem cells (MenSCs). The material was able to control intraoperative hemostasis during a partial hepatectomy, reduce abdominal adhesions, and enhance tissue regeneration through the controlled release of cytokines from the CM. Yu et al. [53] prepared three hydrogen-bonded cross-linked hydrogels via one-step radical polymerization of three bicarboxylic acrylamide monomers. Among them, the N-acryl aspartic acid (AASP) hydrogel showed excellent adhesion properties and effectively sealed the wound and provided emergency hemostasis. Furthermore, PAASP-35%/Fe<sup>3+</sup> hydrogel was fabricated via paper-based ion-transfer printing to form a Janus structure with single-sided adhesion and single-sided antiadhesion properties that could be used to treat gastric perforations in mice. In our previous study [54], we used two precursors: hemostatic sol A<sub>G</sub> (consisting of gelatin and sodium alginate) and antibacterial spray B<sub>S</sub> (consisting of tannic acid and calcium chloride) to form a film in situ at the wound site (Fig. 5F). Physical barrier protection combined with the antibacterial effect of tannic acid provided >98% antibacterial activity and a more stable anti-adhesion effect.

### 5.2. Absorbing or draining biofluids

The biofluids retained in wounds, including blood, tissue fluid, sweat, and other body fluids, easily form a moist environment around the wound, which hinders healing and leads to bacterial growth. Although a waterproof layer on the surface of the dressing can prevent the external environmental fluid from entering the wound, it cannot absorb or remove the internal biological fluid. Zheng et al. [55] prepared biocompatible ultra-long hydroxyapatite (HAP) nanowires and PVA as freeze-dried aerogel. The 3D porous aerogel can absorb a large amount of wound exudate thereby preventing thrombus accumulation and excessive inflammation and slowly releasing active Ca<sup>2+</sup> through HAP; this led to promoting chronic diabetic wound healing in a diabetic mouse model. Shi et al. [56] constructed a wound dressing by electrospinning polyurethane and medical gauze and generated unique fluid self-pumping at the contact point between the hydrophilic cotton fibers and the hydrophobic nanofibers (Fig. 5C). In contrast to the traditional use of the hydrophobic layer in the dressing as an external waterproof layer, the hydrophobic layer in the dressing was used as a contact layer on the wound in practical applications. Xu et al. [57] used hydrophobic

**Table 4**  
Summary of measures to improve sustained effects of hemostatic materials at the site of injury.

Name	Material Components	Improved properties	Main models and hemostasis time	Reference
DCECX/OKGM hydrogels	Dodecyl-modified N-carboxyethyl chitosan, oxidized konjac glucomannan.	Prevent tissue adhesion as physical barrier. Reduce the inflammatory response.	Rat liver resection: 44 ± 7 s	[51]
CM/HC hydrogel	Oxidized hyaluronic acid, glycol chitosan (GC), MenSCs-derived conditioned medium.	Reduce adhesion and enhance tissue regeneration.	Rat liver resection: about 80 s.	[52]
PAASP hydrogels	Aspartic acid, acryloyl chloride, FeCl <sub>3</sub> .	Prevent adhesion and promote wound healing as Janus hydrogel patch.	Rat liver injury: 45 ± 6.5 mg blood loss.	[53]
AgBs-TXA	Gelatin, sodium alginate, tannic acid, calcium chloride.	Antiadhesion as physical barrier and antibacterial effects.	Rat liver injury: about 20 s.	[54]
W-8HAP-2PVA aerogel	Biocompatible inorganic ultralong hydroxyapatite nanowires, polyvinyl alcohol.	Absorb tissue fluid, promote wound healing.	Rat liver puncture: 26.59 ± 7.46 s. Rabbit femoral artery injury: 174.00 ± 16.57 s.	[55]
Self-pumping dressing	Hydrophobic polyurethane nanofiber, hydrophilic cotton medical gauze.	Drain biofluid from wound and promote wound healing.	–	[56]
Janus wound dressing	External hydrophobic adhesive tape, filter paper, polydimethylsiloxane Janus film, amoxicillin powder.	Unidirectionally remove biofluid away from the wound bed. Promote wound healing.	–	[57]
GNPs loaded QC–OA hydrogels	Quaternized chitosan, oxidized sodium alginate, β-Ga <sub>2</sub> O <sub>3</sub> nanoparticles.	Antibacterial, antibiofilm and ROS scavenging.	–	[58]
Ce-MBG/CHT sponge	Mesoporous bioactive glasses, chitosan, Cerium oxide NPs.	Antibacterial (~93.36%).	–	[59]
Ca-TA-MSN@Ag	Mesoporous silica nanoparticles, tannic acid, Ag NPs, Ca <sup>2+</sup> .	Antibacterial (~99 %).	Rat liver injury: 52 ± 6 s. Rat femoral artery: 45 ± 2 s.	[60]
CA-MSN-GTA	Mesoporous silica nanoparticles, cardanol, 2,3-epoxypropyltrimethylammonium chloride.	Antibacterial (~90 %).	Rat femoral artery: 53 s.	[61]
PSLMs	Sodium alginate, cellulose nanocrystal porous microspheres, ε-polylysine.	Antibacterial and wound healing.	Rat liver injury: 48.44 s. Rat femoral artery: 71.66 s.	[62]
BHFs	Alginate, chitosan, collagen-berberine.	Antibacterial and wound healing.	Rat tail amputation: 64.5 ± 18.3 s.	[63]
Portable electrospinning device for outdoor use	CuS composite nanofibers	Ablate superbacteria.	Rat bacterial infection model: <6 s.	[64]
Au@HNTs-chitin composite hydrogel	Au NPs, halloysite nanotubes, chitin.	Antibacterial and wound healing.	Rat liver injury: about 230 s.	[65]
MB@Ker/Alg scaffolds	Alginate, keratin, methylene blue, CaCl <sub>2</sub> .	Antimicrobial photodynamic action.	–	[66]
CA/Ag nanocomposite hydrogel	Ag NPs, <i>n</i> -butylamine and oleic acid, calcium alginate.	Sunlight-sensitive antibacterial without release of Ag <sup>+</sup> , anti-inflammatory.	Rat liver injury: <0.4 g blood loss.	[67]
P-L-MMT hydrogel	Lycium barbarum L. polysaccharide, montmorillonite, polyvinyl alcohol.	anti-inflammatory, wound healing.	Rat liver injury: 76 mg blood loss.	[68]
G-DLPUs	L-arginine, waterborne polyurethane, gelatin methacryloyl.	Wound healing. Enhance vascularization	Rat liver injury: 0.289 g blood loss.	[69]
CS/Ag/TA cryogel	Ag NPs, tannic acid, chitosan	Antibacterial, ROS scavenging, wound healing.	Rat liver injury: <20 s.	[70]
ROS-scavenging hydrogel	pigallocatechin-3-gallate, 2 (hydroxyethyl) methacrylamide, acrylamide, borax.	ROS scavenging, wound healing.	Rat liver injury: <1 g blood loss.	[71]
TXA-MMT Hydrogel@nZnO&MIC	Tranexamic acid, montmorillonite. Zinc oxide NPs, Paeoniflorin, DSPE-TKPEG2k-NH2 copolymer, Aminated gelatin, oxidized dextran.	Cell protection and repairing. Microbe killing. Angiogenic. Healing of chronically infected diabetic wounds.	– Rat liver injury: about 30 s.	[72] [73]
EGF-CM/GelMA	Chitosan microspheres, epidermal growth factor, gelatin methacryloyl.	Wound healing. Accelerating liver regeneration.	Rat liver injury: about 10 s.	[74]
SkinPen	Gelatin methacrylate, Cu-containing bioactive glass nanoparticles.	Wound healing. Angiogenesis, antibacterial.	Rat liver injury: 54.7 ± 16.3 s.	[75]

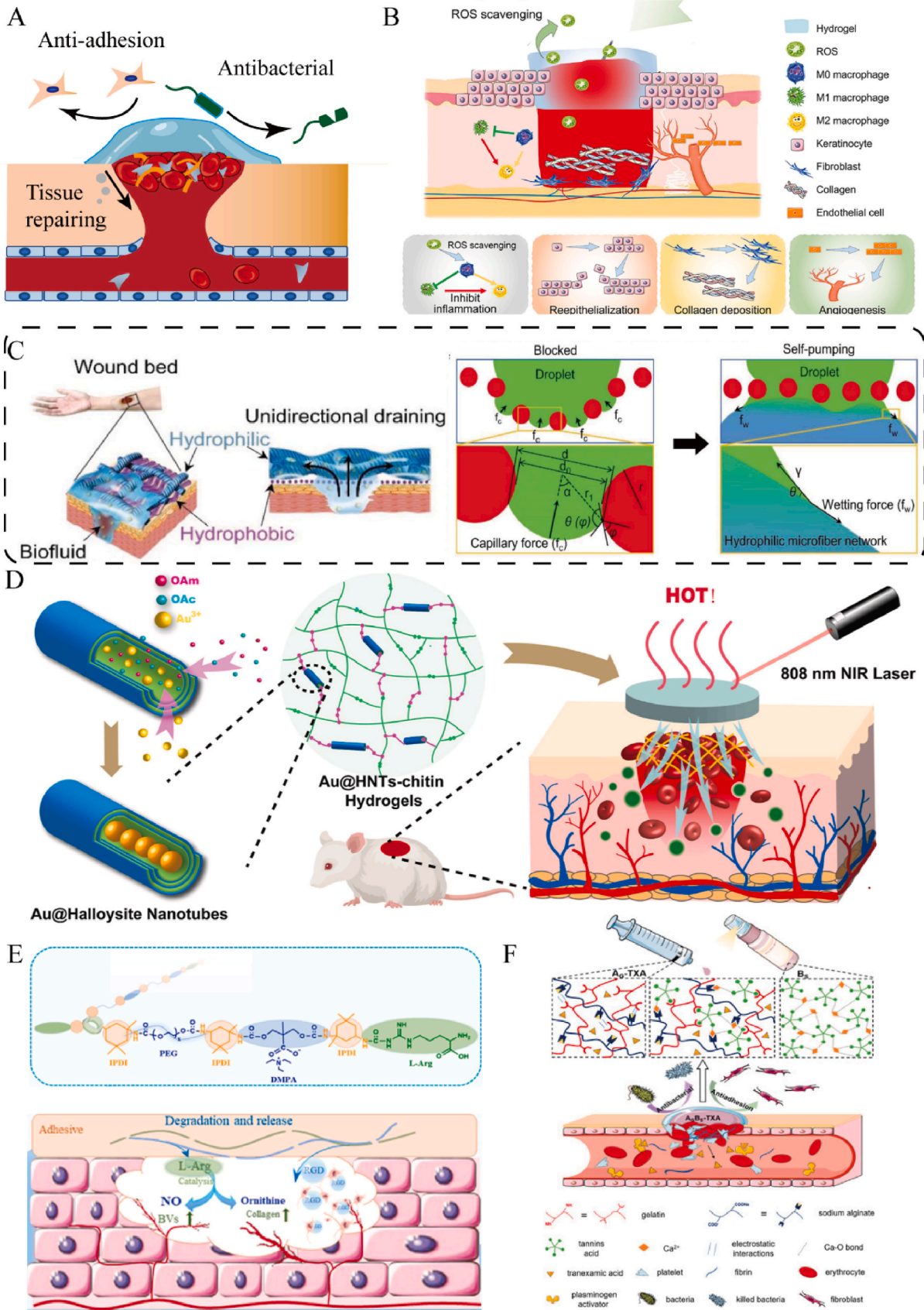
(HP) tape, filter paper, and polydimethylsiloxane (PDMS) to construct Janus structured films exhibiting unidirectional transport of liquid from the hydrophobic side to the hydrophilic side. After draining the biological fluid from the wound, the hydrophobic end still did not adhere to the wound tissue. The authors also explored the ability of stretched or bent dressings to support unidirectional fluid delivery and demonstrated application of such materials on the skin.

The self-pumping structure of the material solved the problems of excessive wound wetting and adhesion of traditional hydrophilic materials after wetting, which increased the efficacy of tissue healing and may be combined with negative pressure drainage technology to expand the scope of clinical application.

### 5.3. Antibacterial treatments

In order to control the wound environment during tissue repair, a number of antibacterial methods have been applied to prevent bacterial adhesion or proliferation, including physical barriers, metal cations/metal nanoparticles, cationic polymers, etc. Negi et al. [58] developed a quaternized chitosan-oxidized sodium alginate hydrogel with β-Ga<sub>2</sub>O<sub>3</sub> nanoparticles loaded as the antibacterial component. The authors believed that the antibacterial property of Ga<sup>3+</sup> is related to its electron configuration and atomic radius which are similar to those of Fe<sup>3+</sup> and affect the survival of bacteria. The quaternized chitosan and β-Ga<sub>2</sub>O<sub>3</sub> nanoparticles in the hydrogel synergistically enhanced the antibacterial effect and targeted the destruction of the bacterial biofilm to kill the bacteria, so no drug resistance occurred. Liu et al. [59] combined the

# Sustained action at the wound of injury



(caption on next page)

**Fig. 5.** Schematic and examples of hemostatic materials' improvement and effect on sustained actions *in vivo*. (A) Schematic of hemostatic materials' sustained actions. (e.g., anti-adhesion, antibacterial, tissue repairing, etc.) (B) EGCG/PHEMAA/PAM hydrogel scavenged ROS to inhibit inflammation and promoted diabetic wound healing. Reproduced under the terms of the CC BY-NC-ND Creative Commons Attribution 4.0 International License. Copyright 2023, published by Elsevier. (C) Schematic of the self-pumping dressing and contact-pumping mechanism, biofluid was drained unidirectionally from the hydrophobic nanofiber array to the hydrophilic microfiber network. Reproduced with permission. Copyright 2018, Wiley-VCH. (D) Schematic showing the preparation process of Au@HNTs and photothermal effect of Au@HNTs-chitin hydrogel to achieve antibacterial and wound healing properties. Reproduced under the terms of the CC BY-NC-ND Creative Commons Attribution 4.0 International License. Copyright 2023, published by Elsevier. (E) Construction of DLPU to achieve sustained release of L-Arg to promote hemostasis and angiogenesis. Reproduced under the terms of the CC BY-NC-ND Creative Commons Attribution 4.0 International License. Copyright 2022, published by Elsevier. (F) Schematic of  $A_2B_8$  hydrogel system, an antibacterial, antiadhesive and smooth film structure was formed when gel was contacted with sol. Reproduced with permission from ACS Applied Materials and Interfaces. Copyright 2023 American Chemical Society.

activation properties of mesoporous bioactive glasses (MBGs) that activate coagulation cascade with the antibacterial properties of cerium oxide nanoparticles to fabricate Ce-MBG/CHT composite sponges. The incorporation of trace elements into the MBG improved its biological activity, which included enhancing its hemostatic and antibacterial effects. Ce-MBG maintained its excellent antibacterial effect through the combined action of particle and ion effects. Chen et al. [60] took advantage of the nature of Janus materials to exert synergistic effects at different stages, and prepared Ca-TA-MSN@Ag particles through redox and coordination reactions. In addition to accelerating hemostasis, the synergistic effect of the released  $Ag^+$  and TA synergism provided 99% antibacterial activity against *Escherichia coli* and *Staphylococcus aureus*. Zhang et al. [61] modified the two sides of anisotropic Janus mesoporous silica nanosheets (MSNS) with cardanol (CA) and 2, 3-epoxypropyltrimethylammonium (GTA) to confer hemostatic and quaternary ammonium cation based antimicrobial functions, respectively. Ouyang et al. [62] used the reverse emulsion method and positive and negative charge self-assembly to prepare SA/CNC@EPL porous hemostatic microspheres (PSLMs). The abundant quaternary ammonium base in  $\epsilon$ -polylysine (EPL) exhibit antibacterial activity similar to those of other positive control drugs. PSLM, which is biodegradable, showed excellent hemostatic effects, provided bacterial control and facilitated tissue repair. Hu et al. [63] prepared SA/CMC/collagen biocomposite hemostatic film with berberine as the main antibacterial component. Berberine can affect the activity of bacteria, especially for Gram-positive bacteria, and inhibits respiration.

To avoid the "super bacteria" problem caused by the excessive application of antibiotics and the biotoxicity problem caused by metal ions, photothermal therapy and photodynamic therapy have been developed as new antibacterial strategies. Liu et al. [64] used portable electrospinning equipment to fabricate CuS composite nanofibers, which were rapidly deposited into wounds outside to stop bleeding, and integrate photothermal destruction of super bacteria and shorten wound healing time. Compared with the traditional electrospun fiber mats, the fibers deposited *in situ* were more compact on rough wound surfaces, providing faster hemostasis and were easier to use in emergency situations. Zhao et al. [65] filled Au NPs in the Halloysite nanotubes (HNTs) to generate photothermal effects, after which the NPs were mixed with chitin to prepare hydrogels. The hydrogel showed superb hemostatic properties and effected photothermal sterilization, which reduced wound infection and promoted rapid healing (Fig. 5D). Furthermore, Feng et al. [66] prepared methylene blue-loaded keratin/alginate composite scaffolds by the cryogel method to mediate antibacterial photodynamic therapy (aPDT) and produce reactive oxygen species (ROS) to effectively combat drug-resistant pathogens. These drug-loaded scaffolds can undergo high-burst release by absorbing wound exudates in the early stages of wound healing and further inhibit bacterial growth to avoid infection. Xu et al. [67] prepared Ag/CA hydrogel, by modifying Ag NPs with oleic acid and *n*-butylamine to form hydrophilic stable colloids. The release of Ag was constrained via cooperation of the hydrogel network and colloids. This design made this hydrogel different from traditional Ag NPs materials, which release the silver ions to provide the antibacterial effect. Under sunlight, hydrogels generate ROS to kill multidrug-resistant bacteria through because of its photodynamic effects, which enables wound healing.

#### 5.4. Tissue repair and wound healing

As mentioned above, the residue of hemostatic materials sometimes affects the healing of wound tissue. In addition to improving the biocompatibility and degradability of materials, the levels of various factors can be regulated during repair can be further regulated to promote tissue healing. Shi et al. [68] applied *Lycium barbarum* polysaccharides to functionalized montmorillonite and then fixed it into polyvinyl alcohol hydrogel. The material inhibited the secretion of inflammatory factors, reduced tissue damage caused by inflammation, reduced the likelihood of wound inflammation, and shortened the wound healing time. Zou et al. [69] added an L-arginine component to the synthetic polyurethane structure, a key mediator in the wound healing process, and regulated the polyurethane structure to make it degradable and enable slow release of L-arginine to promote the vascularization of wound tissue (Fig. 5E). Xu et al. [70] prepared a multifunctional CS/Ag/TA cryogel, in which TA served as a cross-linking agent as well as a reducing agent for Ag NPs, and also scavenged free radicals to facilitate wound tissue repair. The porous structure is another advantage of cryogel, which maintains the mechanical strength of the material as well as creates a comfortable microenvironment for cell proliferation. Jia et al. [71] developed a multifunctional hydrogel capable of ROS-scavenging properties by crosslinking 2-(hydroxyethyl) methacrylamide (HEMAA), acrylamide (AM), and borax with a green tea derivative epigallocatechin-3-gallate (EGCG). In addition to preventing bleeding, the hydrogels scavenged accumulated ROS to protect the cells from ROS-mediated cell death and proliferation inhibition, thereby promoting wound healing (Fig. 5B). Ma et al. [72] prepared an intercalated composite, TXA-MTT, based on montmorillonite (MTT) and tranexamic acid (TXA). The interstitial complex can down-regulated the expression of the inflammatory factors IL-1 $\beta$ , IL-6 and TNF- $\alpha$  and the content of endotoxin induced by radiation, and has potential for use in radiation enteritis and intestinal hemostasis.

In addition, some studies were based on the unique structure of the hemostatic materials themselves, which provide initial environments for wound healing or the introduction of pro-repair factors. Guo et al. [73] designed a hydrogel with on-demand release for refractory diabetic wounds by crosslinking aminated gelatin and oxidized dextran through dynamic Schiff base bonds sensitive to the low pH environments of refractory wounds. Further, nano-ZnO was loaded into the hydrogel to kill microorganisms, and angiogenesis was stimulated by encapsulating peony encapsulated micelles. This sequential response provided healing of chronically infected diabetic wounds. Ding et al. [74] focused on hemostasis and healing of liver injury, and used chitosan microspheres loaded with epidermal growth factor (EGF) and formylated gelatin to prepare *in situ* polymerized hydrogel. EGF played a variety of important roles during tissue healing. Sustained release of the EGF at the wound site after hemostasis enabled hepatocyte proliferation and liver tissue regeneration. Zhou et al. [75] developed a handheld "SkinPen" bioprinter, the hydrogel ink was composed of GelMA and Cu-containing bioactive glass nanoparticles (Cu-BGn), and could strongly adhere to materials when facilitated by ultrasound (US). Cu-BGn endowed the hydrogel with excellent antibacterial and proangiogenic properties. The portability of SkinPen facilitated rapid treatment and management of healing clinical wounds.

## 6. Summary and prospects

Hemostatic materials are often used as auxiliaries in clinical surgery or as quick rescue substitutes in sudden emergencies. The earliest use of cotton gauze and tourniquet suitable for managing bleeding from superficial and compressible wounds, whereas non-compressible bleeding necessitates the use of rapid and potent hemostatic materials. Hydrogels, owing to their injectability and strong adhesive properties, can promptly cover bleeding sites, absorb blood, and seal blood vessels. Hydrogels are particularly suited for use in conjunction with sutures and provide continuous hemostasis and protection for the wound after surgical suturing is completed to avoid postoperative bleeding. The enhanced delivery method enables particle/powder hemostatic materials to swiftly reach deep and narrow bleeding sites like "V" or "J" shape wounds [12], which offers advantages over compressible sponges. For internal bleeding without surface wounds, the intravenous administration of hemostatic materials could achieve hemostasis by targeting the ruptured vessel without additional surgery.

In terms of long-term application, detachable hemostatic materials can alleviate issues caused by misplacement during surgery while facilitating quick dressing changes by medical personnel and reducing patient discomfort during prolonged care. Additionally, there is growing interest in incorporating antibacterial, anti-inflammatory, and pro-repair functions into hemostatic materials as they partially replace the role of wound dressings while providing comprehensive care throughout the healing process.

To further improve the hemostatic effect, composite hemostatic materials involving two or more combinations are the main research direction, for achieving faster hemostasis and covering more application scenarios. Furthermore, many studies have been focused on a variety of effect enhancements beyond hemostasis. However, the complexity and diversity of injuries make it difficult to cover all hemostatic emergencies with one material. The introduction and improvement of new functional groups to improve the treatment efficacy often increase the difficulty of preparing the material, increase the cost, and decrease the stability of the material. Moreover, because of safety considerations, the FDA has approved only certain bioderived materials as hemostatic components. Ways of performing clinical research on materials rapidly, gaining production approval and reaching practical application are also problems to be solved.

In addition, most of the studies cited herein that characterized various properties described are almost separate or independent from the characterization experiments of hemostatic effects, and there are differences between the ideal *in vitro* and *in vivo* environmental conditions, so the parameters obtained under different scenarios may be significantly different, making it difficult to obtain normalized conclusions and develop systematic simulations of hemostatic performance. The currently utilized hemorrhage models, such as rat liver injury, femoral artery injury, and cardiac puncture models, are limited by the blood pressure and total blood volume of small animals. Further research should pay more attention to modeling and testing on large animals, such as pigs or sheep, and modeling of clinical emergencies. For the possible secondary wound bleeding caused by forced movement transported after first aid, Ji et al. [94] designed a dynamic hemostatic model to measure whether hemostatic materials played a role during continuous application. Jia et al. [95] focused on the thermal management of hemostatic materials used in coagulation factors in wounds at high temperature (70 °C) and low temperature (−27 °C) to enable the use of hemostatic materials in extreme environments. The establishment of these models is of great significance for the research on hemostatic materials in more simulated environment and more extreme conditions.

In a recent study, Hou et al. [96] screened different hydrophobic alkyl monomers and catechol adhesion components based on high-throughput screening (HTS) to prepare hydrogels with optimal wet adhesion performance. HTS was used to construct mussel like hydrogels composed of hydrophobic monomers with different alkyl chains and

catechol derivatives at one time, and its wet adhesion properties were optimized and screened. This technology could avoid the traditional time-consuming repeated syntheses for testing and explored the wet adhesion mechanisms of hydrogels based on the results. Furthermore, high-throughput technology can also be used to explore the various biological functions of hydrogels, such as hemostasis and immune regulation. In the field of hemostatic materials, future work may be focused on the establishment of a comprehensive test system for several different specific blood loss models combined with high-throughput characterization, and the screening of multiple indicators to simulate the optimal morphological composition, size, and application scenarios of hemostatic materials.

Future development of hemostatic materials requires the design of multifunctional hemostatic materials that exhibit excellent hemostatic effects, high biocompatibilities, simple production processes, and low production costs. To achieve this goal, it is necessary to focus on various hemostatic mechanisms and effects and enhance and optimize the additional functions needed for practical application. In this review, we outlined four additional functions required of hemostatic materials in addition to hemostasis, and the materials would then be useful in overcoming the challenges encountered in practical applications. We hope that this review will provide a valuable reference for researchers interested in the design and application of hemostatic materials and aid in their development.

### CRedit authorship contribution statement

**Xinran Yang:** Conceptualization, Data curation, Visualization, Writing – original draft. **Xiudan Wang:** Conceptualization, Data curation, Methodology. **Xing Gao:** Resources, Supervision, Investigation, Validation. **Xiaoqin Guo:** Resources, Supervision. **Shike Hou:** Methodology, Resources, Supervision. **Jie Shi:** Methodology, Supervision, Writing – review & editing. **Qi Lv:** Methodology, Supervision, Writing – review & editing.

### Declaration of competing interest

Qi Lv reports financial support was provided by the Opening Project of Military Logistics. Qi Lv reports financial support was provided by National Key R&D Program of China. Qi Lv reports financial support was provided by Tianjin Municipal Natural Science Foundation. If there are other authors, they declare that they have no known competing financial interests or personal relationships that could have appeared to influence the work reported in this paper.

### Data availability

No data was used for the research described in the article.

### Acknowledgements

The authors are very thankful for financial support by National Key R&D Program of China (Grant 2022YFC3006204), Tianjin Natural Science Foundation (20JCYBJC01240), the Opening Project of Military Logistics (No. BLB20J009) and Scientific Research Translational Foundation of Wenzhou Safety (Emergency) Institute of Tianjin University (TJUWYY2022008, TJUWYY2022020).

### References

- [1] D.S. Kauvar, R. Lefering, C.E. Wade, Impact of hemorrhage on trauma outcome: an overview of epidemiology, clinical presentations, and therapeutic considerations, *J. Trauma Acute Care Surg.* 60 (2006) 6, <https://doi.org/10.1097/01.ta.0000199961.02677.19>.
- [2] D.D. Keene, J. Penn-Barwell, P. Wood, N. Hunt, R. Delaney, J. Clasper, R. Russell, P. Mahoney, Died of wounds: a mortality review, *J. Roy. Army Med. Corps* 162 (2016) 5, <https://doi.org/10.1136/jramc-2015-000490>.

- [3] S. Jiang, S. Liu, S. Lau, J. Li, Hemostatic biomaterials to halt non-compressible hemorrhage, *J. Mater. Chem. B* 10 (2022) 37, <https://doi.org/10.1039/D2TB00546H>.
- [4] M. Li, Z. Zhang, Y. Liang, J. He, B. Guo, Multifunctional tissue-adhesive cryogel wound dressing for rapid nonpressing surface hemorrhage and wound repair, *ACS Appl. Mater. Interfaces* 12 (2020) 32, <https://doi.org/10.1021/acsmi.0c08285>.
- [5] S. Wu, Z. Zhang, R. Xu, S. Wei, F. Xiong, W. Cui, B. Li, Y. Xue, H. Xuan, H. Yuan, A spray-filming, tissue-adhesive, and bioactive polysaccharide self-healing hydrogel for skin regeneration, *Mater. Des.* 217 (2022), <https://doi.org/10.1016/j.matdes.2022.110669>.
- [6] G. Pan, F. Li, S. He, W. Li, Q. Wu, J. He, R. Ruan, Z. Xiao, J. Zhang, H. Yang, Mussel- and barnacle cement proteins-inspired dual-bionic bioadhesive with repeatable wet-tissue adhesion, multimodal self-healing, and antibacterial capability for nonpressing hemostasis and promoted wound healing, *Adv. Funct. Mater.* 32 (2022) 25, <https://doi.org/10.1002/adfm.202200908>.
- [7] H. Liu, S. Qin, J. Liu, C. Zhou, Y. Zhu, Y. Yuan, D. Fu, Q. Lv, Y. Song, M. Zou, Z. Wang, L. Wang, Bio-inspired self-hydrophobized sericin adhesive with tough underwater adhesion enables wound healing and fluid leakage sealing, *Adv. Funct. Mater.* 32 (2022) 32, <https://doi.org/10.1002/adfm.202201108>.
- [8] Y. Lu, X. Huang, L. Yuting, R. Zhu, M. Zheng, J. Yang, S. Bai, Silk fibroin-based tough hydrogels with strong underwater adhesion for fast hemostasis and wound sealing, *Biomacromolecules* 24 (2023) 1, <https://doi.org/10.1021/acs.biomac.2c01157>.
- [9] C. Liu, C. Liu, Z. Liu, Z. Shi, S. Liu, X. Wang, X. Wang, F. Huang, Injectable thermogelling bioadhesive chitosan-based hydrogels for efficient hemostasis, *Int. J. Biol. Macromol.* 224 (2023), <https://doi.org/10.1016/j.ijbiomac.2022.10.194>.
- [10] J. Ju, S. Jin, S. Kim, J.H. Choi, H.A. Lee, D. Son, H. Lee, M. Shin, Addressing the shortcomings of polyphenol-derived adhesives: achievement of long shelf life for effective hemostasis, *ACS Appl. Mater. Interfaces* 14 (2022) 22, <https://doi.org/10.1021/acsmi.2c03930>.
- [11] Q. Li, E. Hu, K. Yu, R. Xie, F. Lu, B. Lu, R. Bao, T. Zhao, F. Dai, G. Lan, Self-propelling Janus particles for hemostasis in perforating and irregular wounds with massive hemorrhage, *Adv. Funct. Mater.* 30 (2020) 42, <https://doi.org/10.1002/adfm.202004153>.
- [12] Z. Shi, G. Lan, E. Hu, F. Lu, P. Qian, J. Liu, F. Dai, R. Xie, Targeted delivery of hemostats to complex bleeding wounds with magnetic guidance for instant hemostasis, *Chem. Eng. J.* 427 (2022), <https://doi.org/10.1016/j.cej.2021.130916>.
- [13] M. Yokoyama, N. Chihara, A. Tanaka, Y. Katayama, A. Taruya, Y. Ishida, M. Yuzaki, K. Honda, Y. Nishimura, T. Kondo, T. Akasaka, N. Kato, A biodegradable microneedle sheet for intracorporeal topical hemostasis, *Sci. Rep.* 10 (2020) 1, <https://doi.org/10.1038/s41598-020-75894-w>.
- [14] X. Zhang, G. Chen, L. Cai, Y. Wang, L. Sun, Y. Zhao, Bioinspired pagoda-like microneedle patches with strong fixation and hemostasis capabilities, *Chem. Eng. J.* 414 (2021), <https://doi.org/10.1016/j.cej.2021.128905>.
- [15] R. Haghniaz, H.J. Kim, H. Montazerian, A. Baidya, M. Tavafoghi, Y. Chen, Y. Zhu, S. Karamikamkar, A. Sheikhi, A. Khademhosseini, Tissue adhesive hemostatic microneedle arrays for rapid hemorrhage treatment, *Bioact. Mater.* 23 (2023), <https://doi.org/10.1016/j.bioactmat.2022.08.017>.
- [16] M.K. Klein, H.A. Kassam, R.H. Lee, W. Bergmeier, E.B. Peters, D.C. Gillis, B. R. Dandurand, J.R. Rouan, M.R. Karver, M.D. Struble, T.D. Clemons, L.C. Palmer, B. Gavitt, T.A. Pritts, N.D. Tshilis, S.I. Stupp, M.R. Kibbe, Development of optimized tissue-factor-targeted peptide amphiphile nanofibers to slow noncompressible Torso hemorrhage, *ACS Nano* 14 (2020) 6, <https://doi.org/10.1021/acsnano.9b09243>.
- [17] H. Wang, Y. Zhu, L. Zhang, H. Liu, C. Liu, B. Zhang, Y. Song, Y. Hu, Z. Pang, Nanoplatelets for rapid hemostasis performance, *Chin. Chem. Lett.* 33 (2022) 6, <https://doi.org/10.1016/j.ccl.2021.12.091>.
- [18] Y. Gao, A. Sarode, N. Kokoroskos, A. Ukidve, Z. Zhao, S. Guo, R. Flumenhaft, A. S. Gupta, N. Saillant, S. Mitragotri, A polymer-based systemic hemostatic agent, *Sci. Adv.* 6 (2020) 31, <https://doi.org/10.1126/sciadv.aba0588>.
- [19] G. Bao, Q. Gao, M. Cau, N. Ali-Mohamad, M. Strong, S. Jiang, Z. Yang, A. Valiei, Z. Ma, M. Amabili, Z.H. Gao, L. Mongeau, C. Kastrop, J. Li, Liquid-infused microstructured bioadhesives halt non-compressible hemorrhage, *Nat. Commun.* 13 (2022) 1, <https://doi.org/10.1038/s41467-022-32803-1>.
- [20] W. Han, B. Zhou, K. Yang, X. Xiong, S. Luan, Y. Wang, Z. Xu, P. Lei, Z. Luo, J. Gao, Y. Zhan, G. Chen, L. Liang, R. Wang, S. Li, H. Xu, Biofilm-inspired adhesive and antibacterial hydrogel with tough tissue integration performance for sealing hemostasis and wound healing, *Bioact. Mater.* 5 (2020) 4, <https://doi.org/10.1016/j.bioactmat.2020.05.008>.
- [21] K.P.C. Sekhar, X. Zhang, H. Geng, Q. Yu, P. Zhang, J. Cui, Biomimetic hemostatic powder derived from coacervate-immobilized thermogelling copolymers, *Biomacromolecules* 24 (2023) 11, <https://doi.org/10.1021/acs.biomac.3c00840>.
- [22] X. Zhang, L. Jiang, X. Li, L. Zheng, R. Dang, X. Liu, X. Wang, L. Chen, Y.S. Zhang, J. Zhang, D. Yang, A bioinspired hemostatic powder derived from the skin secretion of *Andrias davidianus* for rapid hemostasis and intraoral wound healing, *Small* 18 (2022) 3, <https://doi.org/10.1002/smll.202101699>.
- [23] G. Wang, X. Meng, P. Wang, X. Wang, G. Liu, D.A. Wang, C. Fan, A catechol bioadhesive for rapid hemostasis and healing of traumatic internal organs and major arteries, *Biomaterials* 291 (2022), <https://doi.org/10.1016/j.biomaterials.2022.121908>.
- [24] X. Peng, X. Xu, Y. Deng, X. Xie, L. Xu, X. Xu, W. Yuan, B. Yang, X. Yang, X. Xia, L. Duan, L. Bian, Ultrafast self-gelling and wet adhesive powder for acute hemostasis and wound healing, *Adv. Funct. Mater.* 31 (2021) 33, <https://doi.org/10.1002/adfm.202102583>.
- [25] V. Krishnadoss, A. Melillo, B. Kanjilal, T. Hannah, E. Ellis, A. Kapetanakis, J. Hazelton, J. San Roman, A. Masoumi, J. Leijten, I. Noshadi, Bioionic liquid conjugation as universal approach to engineer hemostatic bioadhesives, *ACS Appl. Mater. Interfaces* 11 (2019) 42, <https://doi.org/10.1021/acsmi.9b08757>.
- [26] W.C. Huang, Y. He, W. Wang, X. Mao, A biodegradable multifunctional film as a tissue adhesive for instant hemostasis and wound closure, *Macromol. Rapid Commun.* 43 (2022) 9, <https://doi.org/10.1002/marc.202200031>.
- [27] X. Fan, S. Wang, Y. Fang, P. Li, W. Zhou, Z. Wang, M. Chen, H. Liu, Tough polyacrylamide-tannic acid-kaolin adhesive hydrogels for quick hemostatic application, *Mater. Sci. Eng., C* 109 (2020), <https://doi.org/10.1016/j.msec.2020.110649>.
- [28] J.L. Daristotle, S.T. Zaki, L.W. Lau, L. Torres Jr., A. Zografos, P. Srinivasan, O. B. Ayyub, A.D. Sandler, P. Kofinas, Improving the adhesion, flexibility, and hemostatic efficacy of a sprayable polymer blend surgical sealant by incorporating silica particles, *Acta Biomater.* 90 (2019), <https://doi.org/10.1016/j.actbio.2019.04.015>.
- [29] Y. Hong, F. Zhou, Y. Hua, X. Zhang, C. Ni, D. Pan, Y. Zhang, D. Jiang, L. Yang, Q. Lin, Y. Zou, D. Yu, D.E. Arnot, X. Zou, L. Zhu, S. Zhang, H. Ouyang, A strongly adhesive hemostatic hydrogel for the repair of arterial and aortic bleeds, *Nat. Commun.* 10 (2019) 1, <https://doi.org/10.1038/s41467-019-10004-7>.
- [30] Z. Chen, H. Wu, H. Wang, D. Zaldivar-Silva, L. Aguero, Y. Liu, Z. Zhang, Y. Yin, B. Qiu, J. Zhao, X. Lu, S. Wang, An injectable anti-microbial and adhesive hydrogel for the effective noncompressible visceral hemostasis and wound repair, *Mater. Sci. Eng., C* 129 (2021), <https://doi.org/10.1016/j.msec.2021.112422>.
- [31] J. Zhang, Y.-T. Zhao, P.-Y. Hu, J.-J. Liu, X.-F. Liu, M. Hu, Z. Cui, N. Wang, Z. Niu, H.-F. Xiang, Y.-Z. Long, Laparoscopic electrospinning for in situ hemostasis in minimally invasive operation, *Chem. Eng. J.* 395 (2020), <https://doi.org/10.1016/j.cej.2020.125089>.
- [32] Y. Gao, X. Han, J. Chen, Y. Pan, M. Yang, L. Lu, J. Yang, Z. Suo, T. Lu, Hydrogel-mesh composite for wound closure, *Proc. Natl. Acad. Sci. U. S. A.* 118 (2021) 28, <https://doi.org/10.1073/pnas.2103457118>.
- [33] S. Pan, Y. Li, X. Tong, L. Chen, L. Wang, T. Li, Q. Zhang, Strongly-adhesive easily-detachable carboxymethyl cellulose aerogel for noncompressible hemorrhage control, *Carbohydr. Polym.* 301 (2023), <https://doi.org/10.1016/j.carbpol.2022.120324>. Pt B.
- [34] Y. Yang, H. Xu, M. Li, Z. Li, H. Zhang, B. Guo, J. Zhang, Antibacterial conductive UV-blocking adhesion hydrogel dressing with mild on-demand removability accelerated drug-resistant bacteria-infected wound healing, *ACS Appl. Mater. Interfaces* 14 (2022) 37, <https://doi.org/10.1021/acsmi.2c10490>.
- [35] Y. Zheng, K. Shariati, M. Ghovvati, S. Vo, N. Origer, T. Imahori, N. Kaneko, N. Annabi, Hemostatic patch with ultra-strengthened mechanical properties for efficient adhesion to wet surfaces, *Biomaterials* 301 (2023), <https://doi.org/10.1016/j.biomaterials.2023.122240>.
- [36] J. Cao, P. Wu, Q. Cheng, C. He, Y. Chen, J. Zhou, Ultrafast fabrication of self-healing and injectable carboxymethyl chitosan hydrogel dressing for wound healing, *ACS Appl. Mater. Interfaces* 13 (2021) 20, <https://doi.org/10.1021/acsmi.1c02089>.
- [37] Y. Liang, Z. Li, Y. Huang, R. Yu, B. Guo, Dual-dynamic-bond cross-linked antibacterial adhesive hydrogel sealants with on-demand removability for post-wound-closure and infected wound healing, *ACS Nano* 15 (2021) 4, <https://doi.org/10.1021/acsnano.1c00204>.
- [38] X. Wang, Y. Guo, J. Li, M. You, Y. Yu, J. Yang, G. Qin, Q. Chen, Tough wet adhesion of hydrogen-bond-based hydrogel with on-demand debonding and efficient hemostasis, *ACS Appl. Mater. Interfaces* 14 (2022) 31, <https://doi.org/10.1021/acsmi.2c10202>.
- [39] H. Huang, R. Xu, P. Ni, Z. Zhang, C. Sun, H. He, X. Wang, L. Zhang, Z. Liang, H. Liu, Water-driven noninvasively detachable wet tissue adhesives for wound closure, *Mater. Today Bio* 16 (2022), <https://doi.org/10.1016/j.mtbio.2022.100369>.
- [40] R. Xu, S. Ma, Y. Wu, H. Lee, F. Zhou, W. Liu, Adaptive control in lubrication, adhesion, and hemostasis by Chitosan-Catechol-pNIPAM, *Biomater. Sci.* 7 (2019) 9, <https://doi.org/10.1039/c9bm00697d>.
- [41] X. Chen, H. Yuk, J. Wu, C.S. Nabzdyk, X. Zhao, Instant tough bioadhesive with triggerable benign detachment, *Proc. Natl. Acad. Sci. U. S. A.* 117 (2020) 27, <https://doi.org/10.1073/pnas.2006389117>.
- [42] H. He, W. Zhou, J. Gao, F. Wang, S. Wang, Y. Fang, Y. Gao, W. Chen, W. Zhang, Y. Weng, Z. Wang, H. Liu, Efficient, biosafe and tissue adhesive hemostatic cotton gauze with controlled balance of hydrophilicity and hydrophobicity, *Nat. Commun.* 13 (2022) 1, <https://doi.org/10.1038/s41467-022-28209-8>.
- [43] Y. Li, F. Niu, X. Zhao, C.H. Yap, Z. Li, Nonwetting nanostructured hemostatic material for bleeding control with minimal adhesion, *Adv. Mater. Interfac.* 8 (2021) 23, <https://doi.org/10.1002/admi.202101412>.
- [44] W. Li, Y. Zhang, J. Ding, S. Zhang, T. Hu, S. Li, X. An, Y. Ren, Q. Fu, X. Jiang, X. Li, Temperature-triggered fluorocopolymer aggregate coating switching from antibacterial to antifouling and superhydrophobic hemostasis, *Colloids Surf. B Biointerfaces* 215 (2022), <https://doi.org/10.1016/j.colsurfb.2022.112496>.
- [45] J. Shi, D. Wang, H. Wang, X. Yang, S. Gu, Y. Wang, Z. Chen, Y. Chen, J. Gao, L. Yu, J. Ding, An injectable hemostatic PEG-based hydrogel with on-demand dissolution features for emergency care, *Acta Biomater.* 145 (2022), <https://doi.org/10.1016/j.actbio.2022.04.020>.
- [46] Y. Bu, L. Zhang, G. Sun, F. Sun, J. Liu, F. Yang, P. Tang, D. Wu, Tetra-PEG based hydrogel sealants for in vivo visceral hemostasis, *Adv. Mater.* 31 (2019) 28, <https://doi.org/10.1002/adma.201901580>.
- [47] M. Hou, X. Wang, O. Yue, M. Zheng, H. Zhang, X. Liu, Development of a multifunctional injectable temperature-sensitive gelatin-based adhesive double-network hydrogel, *Biomater. Adv.* 134 (2022), <https://doi.org/10.1016/j.msec.2021.112556>.

- [48] Y. He, K. Liu, C. Zhang, S. Guo, R. Chang, F. Guan, M. Yao, Facile preparation of PVA hydrogels with adhesive, self-healing, antimicrobial, and on-demand removable capabilities for rapid hemostasis, *Biomater. Sci.* 10 (2022) 19, <https://doi.org/10.1039/d2bm00891b>.
- [49] M.B. Dowling, I.C. MacIntire, J.C. White, M. Narayan, M.J. Duggan, D.R. King, S. R. Raghavan, Sprayable foams based on an amphiphilic biopolymer for control of hemorrhage without compression, *ACS Biomater. Sci. Eng.* 1 (2015) 6, <https://doi.org/10.1021/acsbomaterials.5b00067>.
- [50] H. Choudhary, M.B. Rudy, M.B. Dowling, S.R. Raghavan, Foams with enhanced rheology for stopping bleeding, *ACS Appl. Mater. Interfaces* 13 (2021) 12, <https://doi.org/10.1021/acsmi.0c22818>.
- [51] X. Wei, C. Cui, C. Fan, T. Wu, Y. Li, X. Zhang, K. Wang, Y. Pang, P. Yao, J. Yang, Injectable hydrogel based on dodecyl-modified N-carboxyethyl chitosan/oxidized konjac glucomannan effectively prevents bleeding and postoperative adhesions after partial hepatectomy, *Int. J. Biol. Macromol.* 199 (2022), <https://doi.org/10.1016/j.ijbiomac.2021.12.193>.
- [52] Z. Li, Y. Zhao, X. Ouyang, Y. Yang, Y. Chen, Q. Luo, Y. Zhang, D. Zhu, X. Yu, L. Li, Biomimetic hybrid hydrogel for hemostasis, adhesion prevention and promoting regeneration after partial liver resection, *Bioact. Mater.* 11 (2022), <https://doi.org/10.1016/j.bioactmat.2021.10.001>.
- [53] J. Yu, Y. Qin, Y. Yang, X. Zhao, Z. Zhang, Q. Zhang, Y. Su, Y. Zhang, Y. Cheng, Robust hydrogel adhesives for emergency rescue and gastric perforation repair, *Bioact. Mater.* 19 (2023), <https://doi.org/10.1016/j.bioactmat.2022.05.010>.
- [54] X. Wang, X. Zhang, X. Yang, X. Guo, Y. Liu, Y. Li, Z. Ding, Y. Teng, S. Hou, J. Shi, Q. Lv, An antibacterial and antiadhesion in situ forming hydrogel with sol-spray system for noncompressible hemostasis, *ACS Appl. Mater. Interfaces* 15 (2023) 1, <https://doi.org/10.1021/acsmi.2c19662>.
- [55] Y. Zheng, W. Ma, Z. Yang, H. Zhang, J. Ma, T. Li, H. Niu, Y. Zhou, Q. Yao, J. Chang, Y. Zhu, C. Wu, An ultralong hydroxyapatite nanowire aerogel for rapid hemostasis and wound healing, *Chem. Eng. J.* 430 (2022), <https://doi.org/10.1016/j.cej.2021.132912>.
- [56] L. Shi, X. Liu, W. Wang, L. Jiang, S. Wang, A self-pumping dressing for draining excessive biofluid around wounds, *Adv. Mater.* 31 (2019) 5, <https://doi.org/10.1002/adma.201804187>.
- [57] B. Xu, A. Li, R. Wang, J. Zhang, Y. Ding, D. Pan, Z. Shen, Elastic Janus film for wound dressings: unidirectional biofluid transport and effectively promoting wound healing, *Adv. Funct. Mater.* 31 (2021) 41, <https://doi.org/10.1002/adfm.202105265>.
- [58] D. Negi, Y. Singh, Gallium oxide nanoparticle-loaded, quaternized chitosan-oxidized sodium alginate hydrogels for treatment of bacteria-infected wounds, *ACS Appl. Nano Mater.* 6 (2023) 14, <https://doi.org/10.1021/acsnm.3c02266>.
- [59] J. Liu, X. Zhou, Y. Zhang, W. Zhu, A. Wang, M. Xu, S. Zhuang, Rapid hemostasis and excellent antibacterial cerium-containing mesoporous bioactive glass/chitosan composite sponge for hemostatic material, *Mater. Today Chem.* 23 (2022), <https://doi.org/10.1016/j.mtchem.2021.100735>.
- [60] J. Chen, L. Qiu, Q. Li, J. Ai, H. Liu, Q. Chen, Rapid hemostasis accompanied by antibacterial action of calcium crosslinking tannic acid-coated mesoporous silica/silver Janus nanoparticles, *Mater. Sci. Eng., C* 123 (2021), <https://doi.org/10.1016/j.msec.2021.111958>.
- [61] Y. Zhang, X. Lu, C. Chi, Y. Zheng, Q. Chen, Sheet-like Janus hemostatic dressings with synergistic effects of cardanol hemostasis and quaternary ammonium salt antibacterial action, *J. Mater. Chem. B* 10 (2022) 45, <https://doi.org/10.1039/d2tb02082c>.
- [62] X.K. Ouyang, L. Zhao, F. Jiang, J. Ling, L.Y. Yang, N. Wang, Cellulose nanocrystal/calcium alginate-based porous microspheres for rapid hemostasis and wound healing, *Carbohydr. Polym.* 293 (2022), <https://doi.org/10.1016/j.carbpol.2022.119688>.
- [63] H. Hu, F. Luo, Q. Zhang, M. Xu, X. Chen, Z. Liu, H. Xu, L. Wang, F. Ye, K. Zhang, B. Chen, S. Zheng, J. Jin, Berberine coated biocomposite hemostatic film based alginate as absorbable biomaterial for wound healing, *Int. J. Biol. Macromol.* 209 (2022), <https://doi.org/10.1016/j.ijbiomac.2022.04.132>. Pt B.
- [64] X.-F. Liu, J. Zhang, J.-J. Liu, Q.-H. Zhou, Z. Liu, P.-Y. Hu, Z. Yuan, S. Ramakrishna, D.-P. Yang, Y.-Z. Long, Bifunctional CuS composite nanofibers via in situ electrospinning for outdoor rapid hemostasis and simultaneous ablating superbug, *Chem. Eng. J.* 401 (2020), <https://doi.org/10.1016/j.cej.2020.126096>.
- [65] P. Zhao, Y. Feng, Y. Zhou, C. Tan, M. Liu, Gold@Halloysite nanotubes-chitin composite hydrogel with antibacterial and hemostatic activity for wound healing, *Bioact. Mater.* 20 (2023), <https://doi.org/10.1016/j.bioactmat.2022.05.035>.
- [66] C.C. Feng, W.F. Lu, Y.C. Liu, T.H. Liu, Y.C. Chen, H.W. Chien, Y. Wei, H.W. Chang, J. Yu, A hemostatic keratin/alginate hydrogel scaffold with methylene blue mediated antimicrobial photodynamic therapy, *J. Mater. Chem. B* 10 (2022) 25, <https://doi.org/10.1039/d2tb00898j>.
- [67] M. Xu, X. Ji, J. Huo, J. Chen, N. Liu, Z. Li, Q. Jia, B. Sun, M. Zhu, P. Li, Nonreleasing AgNP colloids composite hydrogel with potent hemostatic, photodynamic bactericidal and wound healing-promoting properties, *ACS Appl. Mater. Interfaces* 15 (2023) 14, <https://doi.org/10.1021/acsmi.3c03247>.
- [68] S. Shi, X. Lan, J. Feng, Y. Ni, M. Zhu, J. Sun, J. Wang, Hydrogel loading 2D montmorillonite exfoliated by anti-inflammatory Lycium barbarum L. polysaccharides for advanced wound dressing, *Int. J. Biol. Macromol.* 209 (2022), <https://doi.org/10.1016/j.ijbiomac.2022.03.089>. Pt A.
- [69] F. Zou, Y. Wang, Y. Zheng, Y. Xie, H. Zhang, J. Chen, M.I. Hussain, H. Meng, J. Peng, A novel bioactive polyurethane with controlled degradation and L-Arg release used as strong adhesive tissue patch for hemostasis and promoting wound healing, *Bioact. Mater.* 17 (2022), <https://doi.org/10.1016/j.bioactmat.2022.01.009>.
- [70] G. Xu, N. Xu, T. Ren, C. Chen, J. Li, L. Ding, Y. Chen, G. Chen, Z. Li, Y. Yu, Multifunctional chitosan/silver/tannic acid cryogels for hemostasis and wound healing, *Int. J. Biol. Macromol.* 208 (2022), <https://doi.org/10.1016/j.ijbiomac.2022.03.174>.
- [71] G. Jia, Z. Li, H. Le, Z. Jiang, Y. Sun, H. Liu, F. Chang, Green tea derivative-based hydrogel with ROS-scavenging property for accelerating diabetic wound healing, *Mater. Des.* 225 (2023), <https://doi.org/10.1016/j.matdes.2022.111452>.
- [72] F. Ma, S. Sui, Z. Yang, T. Ye, L. Yang, P. Han, H. Gan, Z. Wu, R. Gu, X. Zhu, F. Li, Z. Meng, Z. Jiang, G. Dou, Evaluation of novel tranexamic acid/montmorillonite intercalation composite, as a new type of hemostatic material, *BioMed Res. Int.* 2022 (2022), <https://doi.org/10.1155/2022/3963681>.
- [73] C. Guo, Y. Wu, W. Li, Y. Wang, Q. Kong, Development of a microenvironment-responsive hydrogel promoting chronically infected diabetic wound healing through sequential hemostatic, antibacterial, and angiogenic activities, *ACS Appl. Mater. Interfaces* 14 (2022) 27, <https://doi.org/10.1021/acsmi.2c02725>.
- [74] R. Ding, X. Wei, Y. Liu, Y. Wang, Z. Xing, L. Wang, H. Liu, Y. Fan, Epidermal growth factor-loaded microspheres/hydrogel composite for instant hemostasis and liver regeneration, *Smart Materials in Medicine* 4 (2023), <https://doi.org/10.1016/j.smaim.2022.09.006>.
- [75] F. Zhou, L. Xin, S. Wang, K. Chen, D. Li, S. Wang, Y. Huang, C. Xu, M. Zhou, W. Zhong, H. Wang, T. Chen, J. Song, Portable handheld "SkinPen" loaded with biomaterial ink for in situ wound healing, *ACS Appl. Mater. Interfaces* 15 (2023) 23, <https://doi.org/10.1021/acsmi.3c02825>.
- [76] Y. Ran, E. Hadad, S. Daher, O. Ganor, J. Kohn, Y. Yegorov, C. Bartal, N. Ash, G. Hirschhorn, QuikClot combat gauze use for hemorrhage control in military trauma: January 2009 Israel defense force experience in the Gaza strip—a preliminary report of 14 cases, *Prehospital Disaster Med.* 25 (2010) 6, <https://doi.org/10.1017/S1049023X00008797>.
- [77] M. Pozza, R.W.J. Millner, Celox (chitosan) for haemostasis in massive traumatic bleeding: experience in Afghanistan, *Eur. J. Emerg. Med.* 18 (2011) 1, <https://doi.org/10.1097/mej.0b013e32833a5e4>.
- [78] C. Hoffmann, E. Falzone, T. Martínez, M. Boutonnet, V. Peigne, B. Lenoir, Éponges hémostatiques injectables XStat™ : révolution ou gadget, *Ann. Fr. Anesth. Reanim.* 33 (2014) 11, <https://doi.org/10.1016/j.annfr.2014.07.747>.
- [79] R.J. Ramirez, P.C. Spinella, G.V. Bochicchio, Tranexamic acid update in trauma, *Crit. Care Clin.* 33 (2017) 1, <https://doi.org/10.1016/j.ccc.2016.08.004>.
- [80] R.L. Strausberg, R.P. Link, Protein-based medical adhesives, *Trends Biotechnol.* 8 (1990), [https://doi.org/10.1016/0167-7799\(90\)90134-J](https://doi.org/10.1016/0167-7799(90)90134-J).
- [81] N. Lang, M.J. Pereira, Y. Lee, I. Friehe, N.V. Vasilyev, E.N. Feins, K. Ablasser, E. D. O'Carbhaill, C. Xu, A. Fabbozzo, R. Padera, S. Wasserman, F. Freudenthal, L. S. Ferreira, R. Langer, J.M. Karp, P.J. del Nido, A blood-resistant surgical glue for minimally invasive repair of vessels and heart defects, *Sci. Transl. Med.* 6 (2014) 218, <https://doi.org/10.1126/scitranslmed.3006557>.
- [82] A. Dragu, F. Unglaub, S. Schwarz, J.P. Beier, U. Kneser, A.D. Bach, R.E. Horch, Foreign body reaction after usage of tissue adhesives for skin closure: a case report and review of the literature, *Arch. Orthop. Trauma Surg.* 129 (2009) 2, <https://doi.org/10.1007/s00402-008-0643-5>.
- [83] S. Pourshahrestani, E. Zeimaran, N.A. Kadri, N. Mutlu, A.R. Boccacini, Polymeric hydrogel systems as emerging biomaterial platforms to enable hemostasis and wound healing, *Adv. Healthcare Mater.* 9 (2020) 20, <https://doi.org/10.1002/adhm.202009005>.
- [84] Y. Chan Choi, J.S. Choi, Y.J. Jung, Y.W. Cho, Human gelatin tissue-adhesive hydrogels prepared by enzyme-mediated biosynthesis of DOPA and Fe<sup>3+</sup> ion crosslinking, *J. Mater. Chem. B* 2 (2014) 2, <https://doi.org/10.1039/C3TB20696C>.
- [85] C. Cui, C. Fan, Y. Wu, M. Xiao, T. Wu, D. Zhang, X. Chen, B. Liu, Z. Xu, B. Qu, W. Liu, Water-triggered hyperbranched polymer universal adhesives: from strong underwater adhesion to rapid sealing hemostasis, *Adv. Mater.* 31 (2019) 49, <https://doi.org/10.1002/adma.201905761>.
- [86] Z. Pan, Q.-Q. Fu, M.-H. Wang, H.-L. Gao, L. Dong, P. Zhou, D.-D. Cheng, Y. Chen, D.-H. Qiu, J.-C. He, X. Feng, S.-H. Yu, Designing nanoheavies for rapid, universal, and robust hydrogel adhesion, *Nat. Commun.* 14 (2023) 1, <https://doi.org/10.1038/s41467-023-40753-5>.
- [87] Z. Wang, X. He, T. He, J. Zhao, S. Wang, S. Peng, D. Yang, L. Ye, Polymer network editing of elastomers for robust underwater adhesion and tough bonding to diverse surfaces, *ACS Appl. Mater. Interfaces* 13 (2021) 30, <https://doi.org/10.1021/acsmi.1c09239>.
- [88] J. Saiz-Poseu, J. Mancebo-Aracil, F. Nador, F. Busqué, D. Ruiz-Molina, The chemistry behind catechol-based adhesion, *Angew. Chem. Int. Ed.* 58 (2019) 3, <https://doi.org/10.1002/anie.201801063>.
- [89] J.R. Baylis, J.H. Yeon, M.H. Thomson, A. Kazerooni, X. Wang, A.E. St John, E. B. Lim, D. Chien, A. Lee, J.Q. Zhang, J.M. Piret, L.S. Machan, T.F. Burke, N. J. White, C.J. Kastrup, Self-propelled particles that transport cargo through flowing blood and halt hemorrhage, *Sci. Adv.* 1 (2015) 9, <https://doi.org/10.1126/sciadv.1500379>.
- [90] A. Bal-Ozturk, B. Cecen, M. Avci-Adali, S.N. Topkaya, E. Alarcin, G. Yasayan, Y.-C. E. Li, B. Bulkurcuoglu, A. Akpek, H. Avci, K. Shi, S.R. Shin, S. Hassan, Tissue adhesives: from research to clinical translation, *Nano Today* 36 (2021), <https://doi.org/10.1016/j.nantod.2020.101049>.
- [91] S. Kim, A.U. Regitsky, J. Song, J. Ilavsky, G.H. McKinley, N. Holten-Andersen, In situ mechanical reinforcement of polymer hydrogels via metal-coordinated crosslink mineralization, *Nat. Commun.* 12 (2021) 1, <https://doi.org/10.1038/s41467-021-20953-7>.
- [92] J.-P. Chen, C.-Y. Kuo, W.-L. Lee, Thermo-responsive wound dressings by grafting chitosan and poly(N-isopropylacrylamide) to plasma-induced graft polymerization modified non-woven fabrics, *Appl. Surf. Sci.* 262 (2012), <https://doi.org/10.1016/j.apsusc.2012.02.106>.

- [93] E. Zhang, B. Song, Y. Shi, H. Zhu, X. Han, H. Du, C. Yang, Z. Cao, Fouling-resistant zwitterionic polymers for complete prevention of postoperative adhesion, *Proc. Natl. Acad. Sci. USA* 117 (2020) 50, <https://doi.org/10.1073/pnas.2012491117>.
- [94] W. Ji, S. Li, X. Hou, J. Zhao, X. Yuan, Multiple Non-Covalent Cross-Linked Multifunctional Strong Hemostatic Agent for Dynamic Exposure Hemostasis, *Adv. Healthcare Mater.*, n/a n/a, <https://doi.org/https://doi.org/10.1002/adhm.202302574>.
- [95] X. Jia, C. Hua, F. Yang, X. Li, P. Zhao, F. Zhou, Y. Lu, H. Liang, M. Xing, G. Lyu, Hydrophobic aerogel-modified hemostatic gauze with thermal management performance, *Bioact. Mater.* 26 (2023), <https://doi.org/10.1016/j.bioactmat.2023.02.017>.
- [96] Y. Hou, Y. Li, Y. Li, D. Li, T. Guo, X. Deng, H. Zhang, C. Xie, X. Lu, Tuning water-resistant networks in mussel-inspired hydrogels for robust wet tissue and bioelectronic adhesion, *ACS Nano* 17 (2023) 3, <https://doi.org/10.1021/acsnano.2c11053>.